Mitigating Anthropogenic Climate Change with Aqueous Green Energy: Direct Air Carbon Dioxide Capture and Storage Powered by Ocean Thermal Energy Conversion

by

Sophia Olim

A Thesis Submitted in Partial Fulfillment of the
Requirements of the

HONOURS PROGRAM

in the School of Earth and Ocean Sciences

Supervisors: Andrew Weaver and Michael Eby

We acknowledge and respect the Lək̓ʷəŋən (Songhees and Xʷsepsəm/Esquimalt) Peoples on whose territory the university stands, and the Lək̓ʷəŋən and W̱SÁNEĆ Peoples whose historical relationships with the land continue to this day.

Abstract

In the 2015 Paris Accords, 196 nations agreed to keep global warming below 2°C and to pursue efforts to limit it to below 1.5°C. The Earth has already warmed by around 1.1°C since preindustrial times (Masson-Delmotte et al., 2022; Shukla et al., 2022). If worldwide fossil fuel combustion was immediately eliminated, the direct and indirect net cooling effect of atmospheric aerosol loading would rapidly dissipate. The aerosol cooling realised since the preindustrial era would be eliminated, resulting in an additional warming of around 0.6ºC and taking the Earth rapidly to an around 1.7°C warming. In 2018 the Intergovernmental Panel on Climate Change noted the requirement of widespread negative emissions technology in order to meet this 1.5°C target (Masson-Delmotte et al., 2022; Rumjaun et al., 2018).

In direct air CO_2 capture and storage (DACCS), CO_2 is scrubbed from the atmosphere and injected into underground geological formations (Keith et al., 2018). Carbon dioxide is a potent greenhouse gas and is the focus of many negative emissions technologies. Ocean thermal energy conversion (OTEC) is a form of electricity production that exploits the temperature difference between deep and shallow ocean waters, analogous to land-based heat pumps. OTEC requires a temperature gradient of at least 18ºC and is most efficient in the tropics, due to the high temperature gradient between shallow warm water (around 25 metres deep) and deep cold waters (around 1000 metres deep) (Nihous, 2005). The UVic Earth System Climate Model (UVic ESCM) is used to explore the feasibility of using OTEC to power DACCS as a negative emissions technology in order to help mitigate anthropogenic climate change.

Once this CO_2 has been removed from the atmosphere, it needs to be injected where it can remain safely stored. In marine environments, sedimentary basins along continental shelves, such as depleted oil and gas fields, are the most geologically sound choice for this (Celia et al.,

2015; Strutt et al., 2003). In order to maximise OTEC power production while limiting the need to transport this energy away from the source, offshore OTEC plants are used to power DACCS in two selected oil and gas basins of suitable size in the tropics. OTEC power production of 3 TW of electricity powering DACCS can result in a global relative decrease of 277 parts per million CO_2 by 2100 and a relative temperature decrease of 1.18^{o}C, compared to diagnosed emissions from the IPCC 2018 "business as usual" RCP 8.5 scenario.

There are potential negative impacts to implementing OTEC on a large scale including changes in ocean temperatures, biological productivity, precipitation patterns, and atmosphere-ocean variability (Rau and Baird, 2018; Devault and Péné-Annette, 2017; Rajagopalan and Nihous, 2013; Nihous, 2005). While these must be considered, this combination of green energy and negative emission technology offers an exciting new approach to help mitigate anthropogenic climate change.

Table of Contents

Acknowledgments

I would like to express my deepest gratitude and appreciation to Andrew Weaver and Michael Eby for their constant support, advice, and encouragement throughout this project. I cannot imagine going through this project without the rest of our lab, Anna Nickoloff and Natalia Safianowicz-Gurgacz. I am incredibly grateful for their support, code troubleshooting, and most of all their friendship.

To my parents and brother, I am endlessly grateful for always encouraging my academic pursuits. To my mom for patiently proofreading and my dad for always reminding me basic algebra is harder than calculus - this would not have been possible otherwise.

Finally, I cannot miss the chance to thank my incredible SEOS community of fellow students, professors, and staff. I would not be where I am or who I am today had I not had the opportunity to be a part of such an inspirational, motivational, and gneiss group.

List of Figures

Glossary of Terms

CO_2	Carbon Dioxide
DACCS	Direct Air Carbon Dioxide Capture and Storage
DOW	Deep Ocean Water
EOR	Enhanced Oil Recovery
GHG	Greenhouse Gases
IPCC	Intergovernmental Panel on Climate Change
LCOE	Levelized Cost of Electricity
OTEC	Ocean Thermal Energy Conversion
SOW	Shallow Ocean Water
THC	Thermohaline Circulation

1. Introduction

In the approximately 200 years since the Industrial Revolution, atmospheric CO_2 levels have increased by around 50% due to anthropogenic CO_2 emissions (Masson-Delmotte et al., 2022; Rumjaun et al., 2018). For most of the last millennium, before 1800, atmospheric CO_2 levels were consistently between about 260 and 280 parts per million (ppm) (Masson-Delmotte et al., 2022). In June 2022, CO_2 was measured at 420.99 ppm by the United States National Oceanic and Atmospheric Administration (NOAA) at the Mauna Loa Atmospheric Baseline Observatory (Stein, 2022). The last recorded time in Earth history that has comparable atmospheric CO_2 levels was around 56 million years ago during the Paleocene-Eocene Thermal Maximum, when temperatures were nearly 7°C higher than the modern average (Gingerich, 2019). In order to prevent temperatures from rising this high, in 2015 196 nations signed a legally binding international treaty, agreeing to work together to keep global warming below 2°C and to pursue efforts to limit warming to below 1.5°C (UNFCCC, 2022). This treaty is commonly referred to as the Paris Accords. The Intergovernmental Panel on Climate Change (IPCC) was tasked with producing a report, published in 2018, identifying global emissions pathways consistent with this 1.5°C target. They concluded with high likelihood that the world has likely already warmed by at least 1.1°C (Masson-Delmotte et al., 2022; Rumjaun et al., 2018).

Even if all fossil fuel combustion was immediately eliminated, the world would continue to warm partially due to atmospheric aerosols associated with fossil fuel combustion being scavenged by precipitation (Masson-Delmotte et al., 2022). Aerosols are fine solid or liquid particles that can arise from natural sources, such as volcanic eruptions or sea spray, as well as

human activities and reside suspended in the atmosphere for days to weeks. Aerosols can cool the climate by reflecting incoming sunlight back to outer space (Paynter and Ramaswamy, n.d.). By blocking part of the energy which would otherwise have reached the surface, aerosols cool the climate. It is therefore not surprising that the IPCC report noted the requirement of widespread negative emission technologies in order to meet the 1.5°C target (Rumjaun et al., 2018).

OTEC is a form of marine renewable energy that uses the natural thermal gradient between cold deep ocean water (DOW) and warm surface ocean water (SOW) to power a heat engine (Rau and Baird, 2018). While the basic theory of OTEC is very robust, its application has only been developed in a few pilot plants, including sites in Japan, India, and Hawaii (GESAMP, 2019). Interest in OTEC has continued due to the growing need for clean energy alternatives as the global energy budget increases (GESAMP, 2019; Rajagopalan & Nihous, 2013). In this experiment SOW intake occurs at 25 metres depth, DOW intake occurs at 1000 metres depth, and water is discharged at 25 metres depth. The near surface discharge of cold, nutrient rich water is part of why a global cooling occurs with OTEC use (Nihous, 2005).

In DACCS atmospheric CO_2 is captured, liquidised, and injected into underground geological formations. For long-term CO_2 storage, ocean floor sedimentary basins along passive continental shelves, such as depleted oil and gas fields, are the most geologically sound choice (Celia et al., 2015). In these basins, the liquidised CO_2 is injected into available pore space below an impermeable capstone. Following capture and compression into a supercritical liquid, the carbon dioxide can be injected into underground geologic formations deemed suitable for long term storage. The combination of DACCS and OTEC offers an exciting new approach for independently powered carbon capture plants to inject concentrated supercritical CO_2 into the

deep ocean (Fig. 1). In this project, the UVic Earth System Climate Model (ESCM) is used to explore the use of OTEC as a renewable energy source to power DACCS into selected geological basins in order to help meet the need for negative emission technology to mitigate anthropogenic climate change.

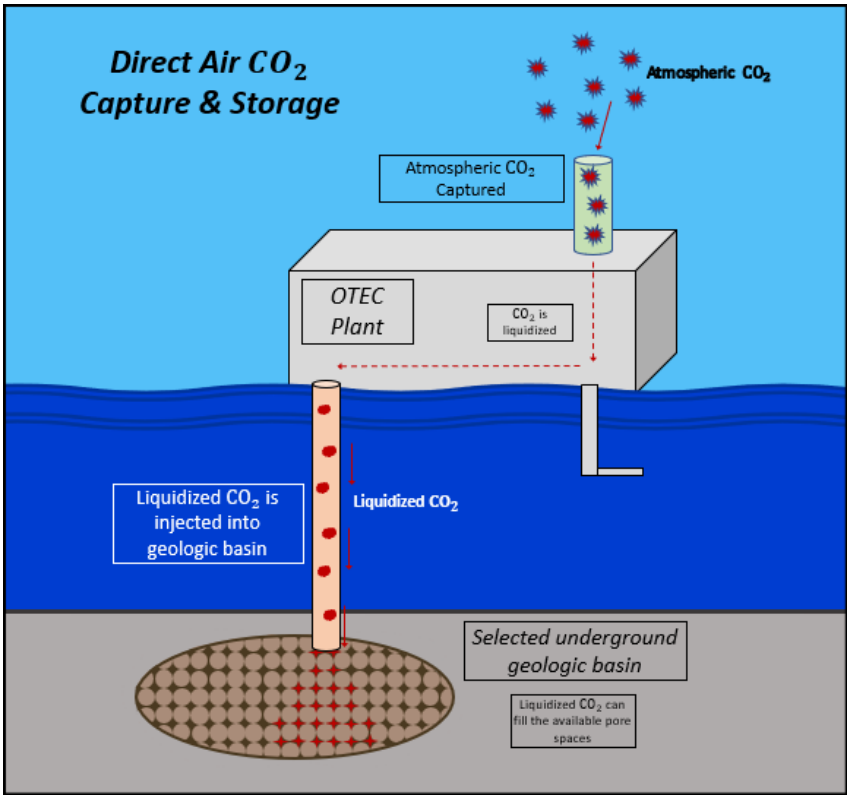

Figure 1: Schematic of simplified combined OTEC and DACCS floating plant.

2. Background

2.1 The Rate of Global Fossil Fuel Emissions

Limiting global warming requires that total cumulative anthropogenic emissions stay within a global total carbon budget.. The carbon budget is the amount of carbon that can be

emitted while keeping global warming below the selected target (Masson-Delmotte et al., 2022). As of 2022, there have already been 2,495 Gigatonnes (Gt) of CO_2 already released since pre-industrial times (Friedlingstein et al., 2022). Reaching net-zero CO_2 emissions by 2050 would require a decrease in CO_2 emissions of approximately 1.4 Gt CO_2 per year from 2022 until 2050. This is about equivalent to the global fall in emissions seen during the 2020 decrease caused by the onset of the COVID-19 pandemic (Friedlingstein et al., 2022).

While the rate of increase in global CO_2 emissions has slowed from 3% per year in the 2000s to 0.5% per year in the 2010s, total global emissions are still growing and in 2022 they were around 40.6 Gt CO_2 (Friedlingstein et al., 2022). The global decrease in the rate of fossil fuel CO_2 emissions can be credited to climate policy and technological changes, including a shift from coal to gas due to reduced expansion of coal capacity and growth in renewable energies (Friedlingstein et al., 2022; Eskander and Fankhauser, 2020; Le Quere et al., 2019).

2.2 The Use of Negative Emissions Technology

Limiting global warming to 1.5ºC or even 2ºC above pre-industrial levels will require unprecedented societal and economic changes to rapidly decrease CO_2 emissions (Masson-Delmotte et al., 2022). The United Nations Framework Convention on Climate Change (UNFCCC) recognizes that for atmospheric greenhouse gases (GHG) levels to stabilise, the rate of anthropogenic GHG additions must be equal to the rate of GHG removal (UNFCCC, 2022). As CO_2 removal from the atmosphere is the opposite of releasing emissions, technology that removes CO_2 is often described as achieving “negative emissions” (de Coninck et al., 2018).

Increased atmospheric CO_2 removal can be achieved either by enhancing natural processes that act as CO_2 sinks (including increasing uptake by trees, soil, or the ocean surface) or through man-made processes (including the direct capture of atmospheric CO_2 followed by

underground storage) (de Coninck et al., 2018). At present levels, removal by natural systems cannot keep up with the rate of anthropogenic GHG emissions. Removing CO_2 from ambient air was first commercialised in the 1950s for the use as a pre-treatment for cryogenic air separation (Keith et al., 2018). It was not until the 1990s that Klaus Lackner began exploring large-scale CO_2 capture in order to mitigate risk from anthropogenic climate change (Lackner et al., 1999).

3. The Use of Geoengineering

3.1 Geologic CO_2 Storage

Geologic CO_2 storage occurs when, after being captured by direct air or another carbon capture process, CO_2 is stored in deep underground geologic formations (Stevens et al., 2001) (Fig. 2). This can be done on terrestrial land or underwater in various geologic settings, including basalt formations, saline aquifers, and sedimentary rocks. This method of carbon injection is sometimes part of enhanced oil recovery (EOR), where liquid CO_2 is injected into the oil-bearing formation to lower the viscosity of the oil, therefore allowing the oil to flow more easily to the oil well (Stevens et al., 2001). Currently a few plants around the world, including ones in British Columbia and Iceland, use direct air capture technology to capture atmospheric CO_2 then inject the liquidised CO_2 into long term deep geologic storage (Carbon Engineering Ltd., 2023). In the 2005 *IPCC Special Report on Carbon dioxide Capture and Storage*, the IPCC concluded that when storage sites are properly selected and regulated, CO_2 can be stored for millions of years with very low risk (Metz et al., 2005).

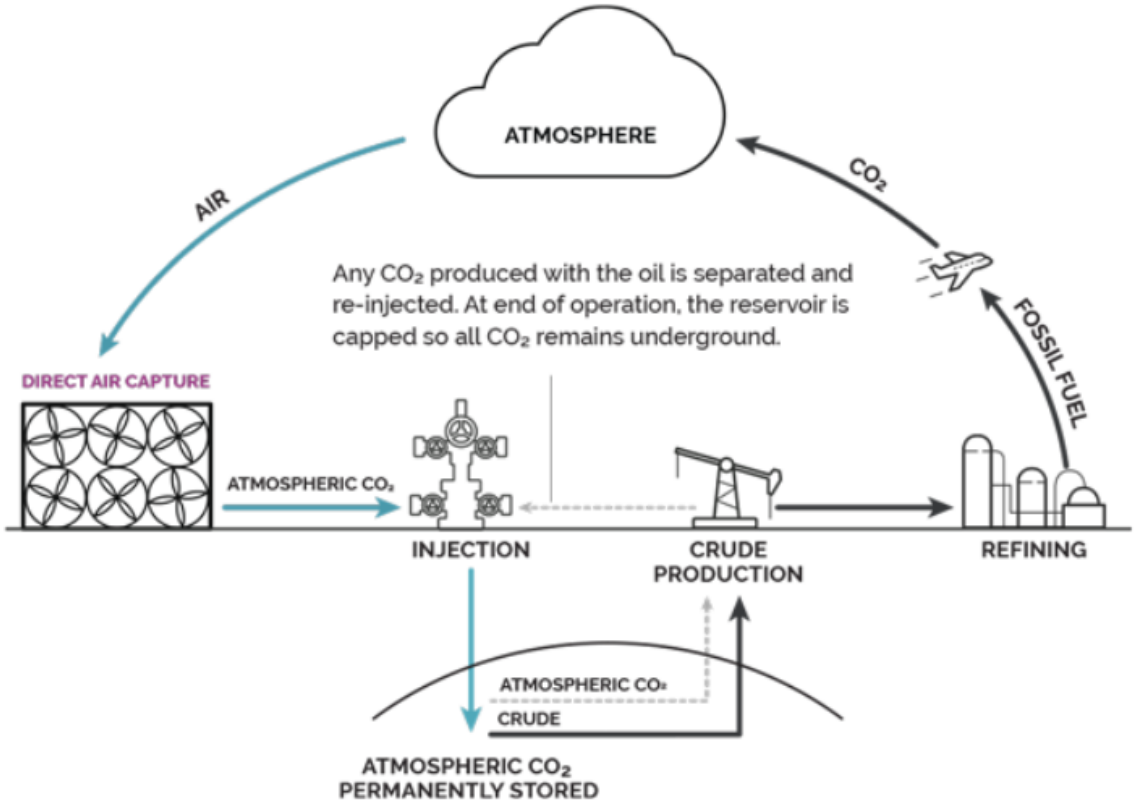

Figure 2: *Schematic of Direct Air CO_2 Capture and Storage process. Taken from Carbon Engineering Ltd. (2023).*

The long term storage of CO_2 in deep geologic formations is not a manmade concept, but rather a widespread geologic occurrence (Benson et al., 2018). Carbon dioxide can become naturally trapped in underground reservoirs and remain there for centuries or longer (Benson et al., 2018). These natural CO_2 storage sites are well studied by the oil and gas industry (Metz et al., 2005). Below depths of 800 to 1000 metres, the density of supercritical CO_2 is liquid-like at 250 to 800 kg / m^3 (Benson et al., 2018; Celia et al., 2015). This density is significantly lower than the density of water or brine and allows significant mass to be stored per unit pore space (Celia et al., 2015). The CO_2 remains trapped in the rock for a number of reasons including: dissolution in the situ formation fluids, trapping of CO_2 below a confining layer (an impermeable

caprock), retention when trapped in available pore spaces, adsorption onto the pre-existing organic matter, or reaction with the minerals in the storage formation to produce carbonate minerals (Benson et al., 2018).

3.1.1 Choosing Appropriate Areas for Long Term CO_2 Storage

The conditions needed for CO_2 to become entrapped in pore spaces where it will remain for long periods of time are generally met by sedimentary rocks (Celia et al., 2015). Metamorphic and crystalline rocks are not suitable for CO_2 storage due to their low porosity, low permeability, and high fracture rate. Injection formations for CO_2 must meet three conditions: the ability to accept injected CO_2, a high enough capacity to store the intended amount of CO_2 and well established containment so that no, or essentially no, CO_2 leaks out from the injection site. The impermeable capstones are critical for long term storage, as they form the barrier to keep CO_2 from leaving the injection site. Suitable capstone rocks include shales, anhydrides, and salt beds that are not faulted or fractured to the point of fluid leakage (Celia et al., 2015).

The potential for long term storage at the selected geologic sites must be large when compared to annual emissions in order to have a significant effect as a negative emissions technology (on the order of Gt of CO_2 a year). Depleted oil and gas fields make ideal sites for long term carbon dioxide storage due to existing geologic data proving these areas have good storage and trapping characteristics (Carbon Engineering, 2023). While there is also extensive research on injection into oceanic basalt sites and deep saline formations, this research project focuses on injection into proven oil and gas reserves in hydrocarbon producing sedimentary basins. This is because the structures of oil and gas sites are already well known, which would reduce the time and money needed for determining if these are suitable sites (Benson et al., 2018).

The injection of CO_2 into depleted oil and gas reserves could be done using very similar technology to that used by oil and gas companies for the production of hydrocarbons and underground waste injection (Metz et al., 2005). The technology for injecting CO_2 underground has been proven and practised by the oil and gas industry for enhanced oil recovery since the 1970s (Stevens and Gale, 2000; IPCC, 2000; Blunt et al., 1993). While the numerous wells already penetrating capstones at proven oil and gas sites do present possible leakage sites, utilising existing locations would decrease the cost to create new wells (Fig. 3) (Benson et al., 2018).

Additionally since these already known wells would be the main possible points of leakage across the injection site, they could be monitored to ensure little leakage occurs (Benson et al., 2018). Monitoring technology developed by the oil and gas industry can also be used at these sites. Monitoring techniques developed in order to determine the scope of potential oil and gas reservoirs, such as seismic surveys, have been proven adequate for observing underground CO_2 injection sites (World Oceans Review, 2010; Metz et al., 2005; Gale et al., 2001). While it can generally be assumed that CO_2 storage will occur after oil and gas reservoirs are depleted, storage combined with enhanced oil and gas recovery is an option for CO_2 storage in basins that are not depleted (Benson et al., 2018).

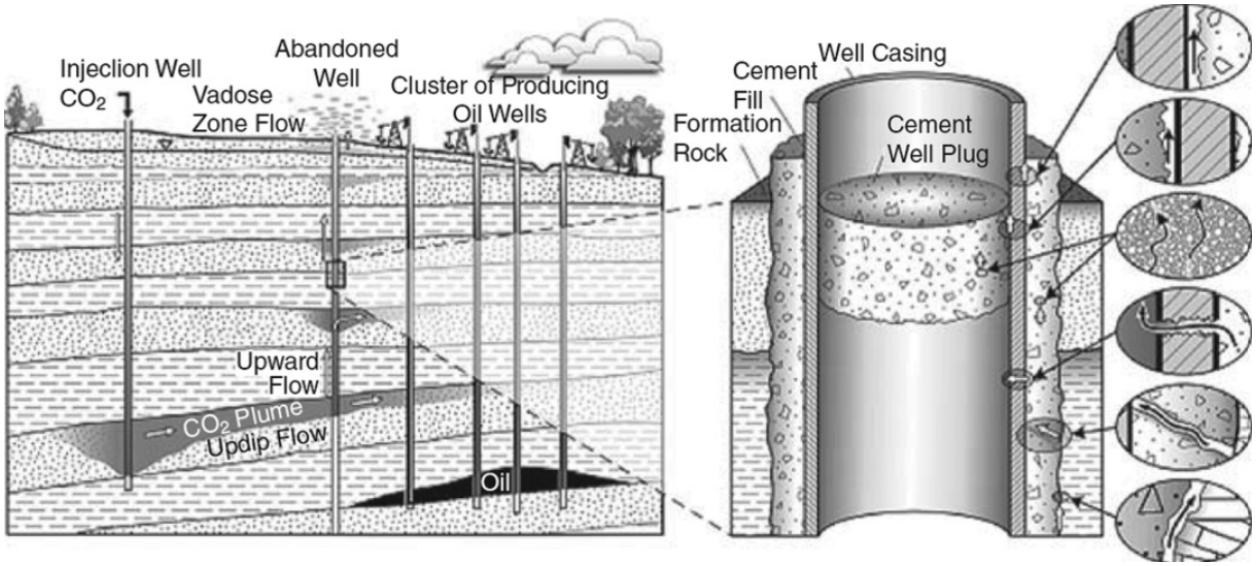

Figure 3*: Schematic of CO_2 injection into a formation that includes a number of old oil and gas wells. Figure from Nordbotten and Celia (2012), modified from Gasda et al. (2004).*

Current CO_2 storage projects demonstrate that monitoring is able to detect movement of CO_2 in reservoirs (Benson et al., 2018). No releases of CO_2 to the surface have been detected, but it must be noted that these projects have a comparatively short history and there are not many sites (Whittaker, 2005; Chadwick et al., 2005). Measurements from enhanced oil recovery (EOR) projects, where more than 100 Mt CO_2 has been injected into various sites, suggest that the fractional CO_2 release rates are zero (Klusman, 2003; Moritis, 2002). While it is difficult to exactly measure capacity for CO_2 storage, it is estimated that depleted oil and gas reservoirs globally would have a storage capacity of 675 to 900 $GtCO_2$ (Benson et al., 2018).

It is considered likely that injection of CO_2 into carefully selected storage sites can result in CO_2 retention of 99% or more for at least 1000 years (Benson et al., 2018). While there are some suggestions of co-storage of CO_2 along with hydrogen sulphide, sulphur dioxide, or nitrogen dioxide, there is limited information about whether the economic value of this would outweigh the additional questions that would arise regarding transport and storage of these mixed constituents. Therefore, this report considers only the storage of CO_2.

3.1.2 The Cost of CO_2 Storage in Deep Marine Sites

Since large CO_2 leakages at these deep sites have the potential to be catastrophic for the deep sea environment, careful monitoring is needed to prevent leakage and if it does occur, to mitigate as fast as possible. Oil and gas industries already have many comprehensive site monitoring programs in place that could be used. As of 2018, the price of monitoring these sites is around 0.6 to 0.8 USD_{2018} per tonne CO_2 stored (Benson et al., 2018). The price for CO_2 sequestration in offshore depleted oil and gas fields is very site specific and ranges from 0.5 to 8.1 USD_{2018} per tonne CO_2 stored (Benson et al., 2018).

3.2 Direct Air Carbon Dioxide Capture and Storage

Carbon dioxide capture can be achieved by capturing CO_2 arising directly from the combustion or preparation of fossil fuels (as in power generation or natural-gas processing), from the combustion of biomass based fuels, from certain industrial processes (such as cement production), or directly from the air (Metz et al., 2005). Once the gases are captured, the CO_2 must be separated from other gases prior to transportation to a storage site. While technology capable of scrubbing CO_2 from a gas stream using chemical solvent was developed in the 1940s, its use as part of climate change mitigation was first recorded in 1982 (Siddique, 1990; Horn and Steinberg, 1982). Horn and Steinberg first investigated CO_2 separation as a method to generate electricity (Siddique, 1990; Horn and Steinberg, 1982). In 1996 Audus et al. discussed the addition of long-term storage following CO_2 capture. Prior to transportation to geologic storage sites, CO_2 must be compressed so that its volume is reduced to around 0.2% of its gaseous volume. As several million tonnes of CO_2 are transported by pipeline a year, there is already existing technology for transportation to geologic sites (Skovholt, 1993).

Direct air carbon capture and storage (DACCS) is a tool that in the short term can be used to accelerate the rate at which societies can reach net-zero emissions. Artificially removing some of the CO_2 already present in the atmosphere also gives societies more leeway in future greenhouse gas (GHG) emission reductions. In the future, if global net-zero is reached, DACCS can be used to reduce global atmospheric CO_2 (Rumjaun et al., 2018). As of the 2005 *IPCC Special Report on Carbon Dioxide Capture and Storage*, in order to achieve stabilisation of 550 parts per million by volume there will need to be global emissions reductions of around 38 $GtCO_2$ per year.

The work of Carbon Engineering in Squamish, British Columbia is based on industrial large scale capture of atmospheric CO_2 with components drawn from well-established commercial direct air carbon dioxide capture (DACC) techniques and reflects decades of development. Recent numbers suggest that 366 kWh is needed to provide energy to capture and sequester one tonne CO_2 (Keith et al., 2018). Each OTEC plant in this modelling study is capable of producing 100 MW per year. Therefore, one OTEC plant producing 100 MW of electricity could capture and sequester about 21,541 tonnes CO_2 per year (Eq. 1).

$$\left(\frac{1\ tonne\ CO_2}{366\ kWh}\right)\left(\frac{10^3\ kW}{1\ MW}\right)\left(\frac{8760\ hr}{1\ yr}\right) = 23{,}934.43\ tonnes\ CO_2\ /\ yr \quad \text{(Eq. 1)}$$

3.2.1 The Cost of DACCS

One of the major factors in determining the cost of DACCS is the cost of energy used to power the system. Since the "energy requirement for CCS [carbon dioxide capture and storage] is substantially larger than for other emission control systems" (Allam et al., 2018), how

DACCS is powered is an important consideration to ensure the process is both economically and environmentally profitable.

Estimates of the cost of direct air capture technology varies widely with cost estimates based in simple scaling relationships, yielding results from 20 to 1,000 USD_{2018} per tonne CO_2 (de Coninck et al., 2018; Keith et al., 2018; Johnson et al., 2017; Lackner, 2016; Socolow, 2011; House et al., 2011; Lackner et al., 2012). There are many factors and low levels of agreement on the cost of DACCS and it is often compared relative to other negative emissions technologies (Fig. 4) (de Coninck et al., 2018). The IPCC suggests four factors to consider in the cost of CO_2 capture: capital cost, incremental product cost, cost of CO_2 captured, and cost of CO_2 avoided (de Coninck et al., 2018).

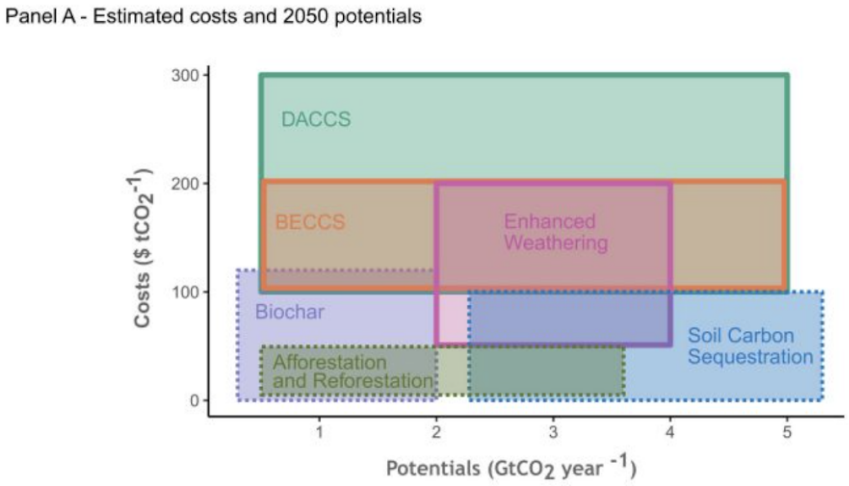

Figure 4: *Panel A presents estimates of costs in USD / tonne CO_2 compared to potential capacity in Gt CO_2 / year for various negative emissions technologies based on a systematic review of the bottom up literature. DACCS – direct air carbon dioxide capture and storage; BECCS – bioenergy with carbon capture and storage. Dashed lines display saturation limits for the corresponding technology. Reference year for all potential estimates is 2050, while all cost estimates preceding 2050 have been included (as early as 2030, older estimates are excluded if they lack a base year and thus cannot be made comparable). Costs refer only to abatement costs. Taken from de Coninck et al. (2018).*

The Capital Cost

The capital cost is used to measure the total spending needed for the design, purchase, and installation of the system of interest (Allam et al., 2018). For CO_2 capture systems the capital cost is usually reported on a normalised basis (e.g. money per kW). The IPCC 2018 considers the cost of CO_2 capture for a selected energy plant to be the difference between what it would cost to build the plant with CO_2 capture versus without CO_2 capture, while the plant produces the same amount of useful primary product (Allam et al., 2018). In 2018, Carbon Engineering provided a paper that provided a design and engineering cost basis for an aqueous DACC system by drawing from "well established commercial engineering heritage" and when need be "described in sufficient detail to allow assessment by third parties." The Carbon Engineering aqueous DACC system, which Carbon Engineering has worked on since 2009, captures CO_2 from the atmosphere using an aqueous alkali capture fluid along with a calcium loop to drive the removal of a carbonate ion (Keith et al., 2018).

Carbon Engineering estimated the capital cost of an early plant with the capacity of drawing down 0.98 Mt CO_2 a year at \$1,126.8 million USD_{2016} , with the cost predicted to lower to \$779.5 million USD_{2016} (Keith et al., 2018). This is based on the assumption that as plant production increases it will be linearized, with non-field costs (such as engineering) and indirect field costs (such as construction supervision and start-up costs) decreasing. This capital cost estimation matches that of the 2011 American Physical Society estimate on DACC costs (Socolow et al., 2011).

The Incremental Product Cost

One of the critical measures of the economic impact of DACC is the cost of electricity (COE). While there are many variables at play in calculating the LCOE, Keith et al. (2018)

estimate a levelized cost of \$94 to \$232 USD_{2018} per tonne CO_2 captured and sequestered. This is based on energy costs, financial assumptions, and engineering decisions. They consider levelized costs per tonne CO_2 to be comprised of the capital cost, non-fuel operations and maintenance, and energy costs. In 2018 Carbon Engineering assumed a natural gas cost of 3.5 USD_{2018} / GJ and electricity costs of 30 and 60 USD_{2018} / MWh. The full breakdown of choices for the Carbon Engineering DACCS plant can be found in Keith et al. (2018).

The Cost of CO_2 Captured

The cost of CO_2 captured or removed is based on the mass of CO_2 removed. This is done to take into account the economic viability of a CO_2 capture system while considering CO_2 to be an industrial commodity (Allam et al., 2018). By considering the economic viability of a CO_2 capture system with the market price of CO_2, the COE for a plant using DAC would be equal to that of a plant without DAC technology. The cost of CO_2 captured can be calculated by subtracting the COE of a reference plant without DAC technology from the COE of a plant with DAC, then dividing this by the total mass of CO_2 captured per net kWh.

The Cost of CO_2 Avoided

The cost of CO_2 emissions avoided is one of the most commonly used measures for the cost of DACCS (Allam et al., 2018). This is calculated based on the average cost of reducing atmospheric CO_2 emissions while providing the same amount of primary reference product as a plant without DACCS. This can be found by subtracting the COE of a reference plant from the COE of a plant with DACCS, subtracting the mass emission rate of CO_2 / kWh generated of a reference plant from that of a plant with DACCS, then dividing the former by the latter (Allam et al., 2018). This method of calculation is particularly useful as it can be used to compare any two systems of interest.

3.3 Ocean Thermal Energy Conversion

The idea of OTEC was first considered over 150 years ago in Jules Verne's "Twenty Thousand Leagues Under the Sea" (GESAMP, 2019). In 1881, nearly ten years after the main character Captain Nemo proposed producing electricity using the ocean thermal gradient, OTEC was first suggested as a viable process for renewable energy generation (Vega, 2016; d'Arsonval, 1881). While initial and ongoing studies consider OTEC primarily as a way to generate clean electricity, more recently OTEC has been considered as an energy source for CO_2 negative emissions technology (GESAMP, 2019; Rau and Baird, 2018). OTEC also may indirectly sequester CO_2 by bringing up nutrient rich DOW to the surface ocean, therefore increasing primary production (Yool et al., 2009). However DOW will also contain elevated CO_2 compared to SOW, and as such the surface air-sea CO_2 uptake gradient will lead to reducing the ocean CO_2 uptake (GESAMP, 2019).

The heat engine technology used in OTEC is very common in thermal power plants today (Rajagopalan and Nihous, 2013). As common as this technology is, the implementation of OTEC faces many problems, including reliance on ocean thermal gradients larger than those of that needed for other analogous technology, the technology's low thermodynamic efficiency (around 3%), and the need to move very large amounts of water to produce a worthwhile amount of electricity (Nihous, 2005). The OTEC power generation process requires the use of a working fluid, which can be either another fluid with a low boiling point or ocean water (Vega, 1995). OTEC plants require a temperature gradient between SOW and DOW of at least 18^{o}C but are more efficient in areas with higher temperature gradients (Nihous, 2005). Locations with large enough temperature gradients are largely restricted to the tropics (Fig. 5) (GESAMP, 2019; Devault and Péné-Annette, 2017; Faizal and Ahmed, 2013).

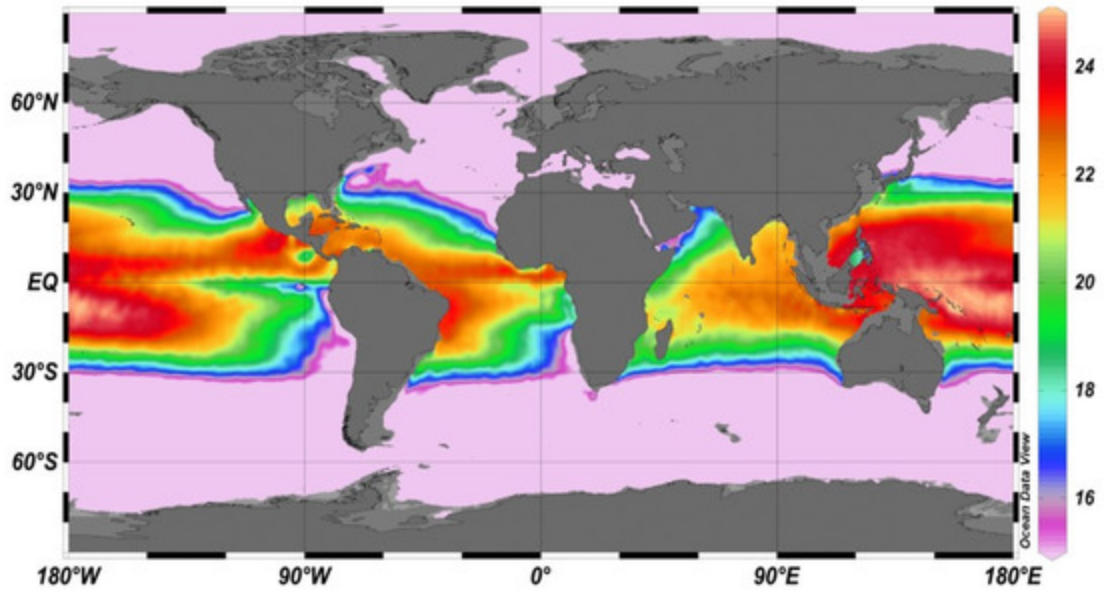

Figure 5: *Distribution of annual average temperature differences between 1000m deep water and surface waters. Colours warmer than light blue represent areas where there is a sufficiently large temperature gradient to support OTEC (greater than 18 ºC). Taken from Nihous (2018).*

There are three types of OTEC systems: closed cycle systems (CC-OTEC), open cycle systems (OC-OTEC), and hybrid systems (Vega, 1995). In CC-OTEC the working fluid, commonly anhydrous ammonia, is evaporated under pressure using heat from the warm SOW (Fig. 6). The steam from this is used to power a turbine-generator to produce electricity (Wang et al., 2008). In OC-OTEC the seawater is flash evaporated in a vacuum chamber. This produces a low power system that drives a turbine, generating electricity (Fig. 7) (Vega, 1995). In hybrid systems warm SOW enters a vacuum chamber where it is evaporated into steam. This steam then vaporises ammonia, which drives the turbine to produce electricity. Upon condensation of the steam within the heat exchanger, desalinated water is produced as a by-product (Vega, 1999). This desalinated water could be of great help to areas that already struggle to obtain sufficient freshwater, particularly small island developing nations around the equator.

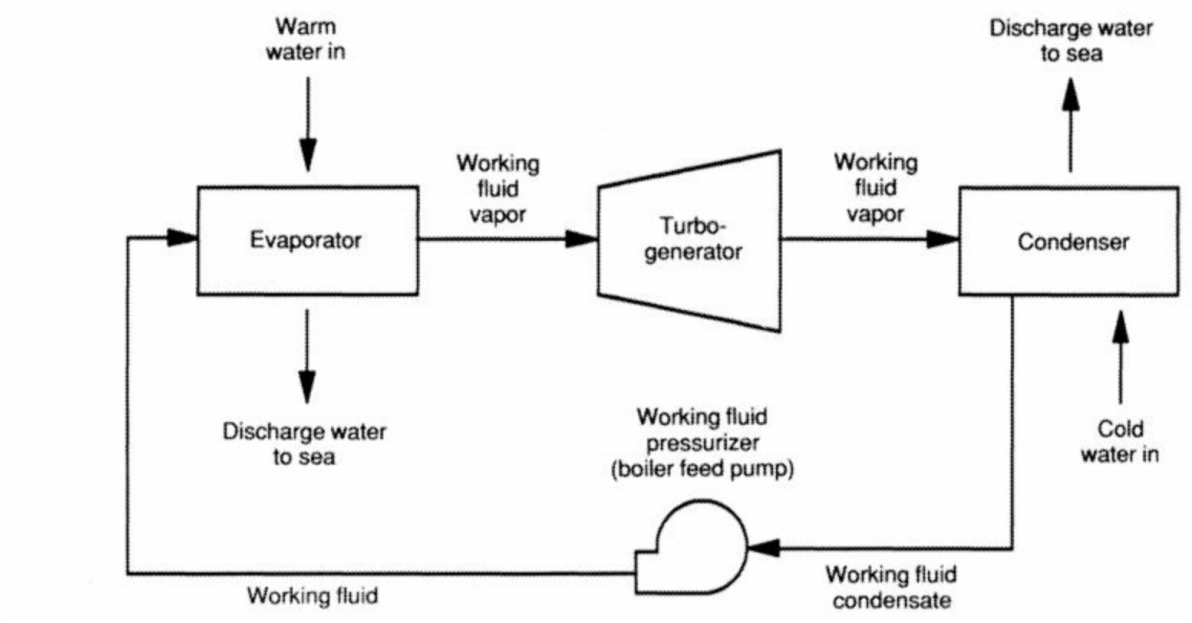

Figure 6: *Schematic of an offshore CC-OTEC Plant. Image taken from the U.S. Department of Energy (2023).*

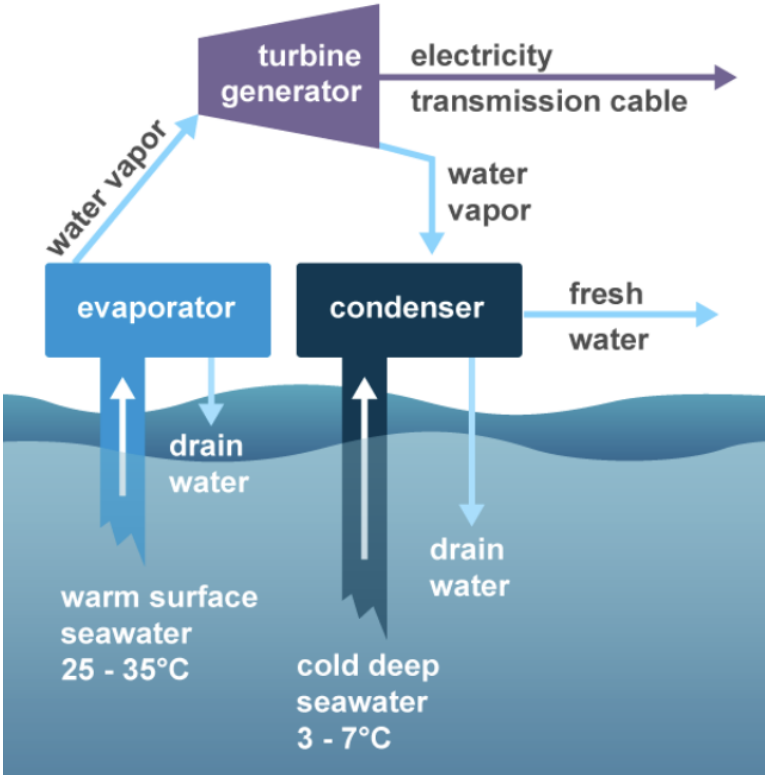

Figure 7: *Schematic of an offshore CC-OTEC Plant. Image taken from the US Energy Information Administration (2022).*

Approximations of how much power OTEC is able to produce per year without significantly degrading the ecosystem vary greatly from 3 Terawatts (TW) (Nihous, 2018) to 1000 TW (Vega, 1995). The discrepancy comes from the large amount of uncertainty surrounding the limiting factor for reservoir renewal. The more conservative estimates, less than 50 TW per year, take into consideration factors including deep water formation (Johnson, 1992), environmentally safe levels of OTEC production density (Avery and Wu, 1994), and possible disruptions from OTEC of the oceanic thermohaline circulation (THC) (Rau and Baird, 2018; Nihous, 2018). The larger estimates largely only consider very broad factors such as oceanic evaporation rates and insolation (Masutani and Takahashi, 2000; Vega, 1995).

3.3.1 The Environmental Impacts of OTEC

Physical

One of the main concerns for physical impacts from OTEC is the disruption of the THC. The THC plays a critical role in regulating global climate (Rajagopalan and Nihous, 2013). While it is not definitively known how OTEC would affect the THC, some researchers predict that implementing OTEC would result in a strengthening of the THC (Rau and Baird, 2018; Rajagopalan and Nihous, 2013). This strengthening is attributed to the increase in turbulent mixing that would result from OTEC. As OTEC pumping increases, the plants draw more water from the water column, which decreases the density stability and increases turbulent mixing.

Another key concern from OTEC implementation is its effect on ocean surface water temperatures. The ocean surface plays a critical part in regulating the global climate. Global processes controlled or greatly affected by sea surface temperatures include on-land carbon cycling in coastal ecosystems, air-sea gas exchange, ocean primary productivity, and coastal wind patterns (Bolles, 2023). OTEC results in a decrease in ocean sea surface temperatures

relative to a scenario without OTEC. This is partially due to the introduction of large volumes of cold DOW to the surface from the resultant artificial upwelling. However, despite this, sea surface waters will continue to warm due to large-scale global warming over the next few centuries. In scenarios with OTEC, this sea surface warming occurs at a slower rate than in any scenario without OTEC. Research suggests both a decrease in sea surface warming rate and a strengthening of the THC with increased OTEC production.

Biological

Both the construction and the physical presence of OTEC plants will affect local biota. Processes that will affect these organisms include impingement, where organisms and particles are trapped within a structure or on a surface due to water flow; entrainment, where organisms and particles enter the water intake into the OTEC plant structure; habitat displacement; noise and light pollution; increased local water turbidity; and effects from the use of biocides (Devault and Péné-Annette, 2017). Entrainment and impingement are almost certainly fatal to the biota. The accumulation of biota on the surfaces of OTEC pipes will also decrease the efficiency of the plant (Devault and Péné-Annette, 2017). Anti-fouling biocides are used to remove this accumulation to maintain the efficiency of OTEC plants, but in large amounts these agents may have a negative impact on the surrounding ecosystem (Devault and Péné-Annette, 2017).

Since OTEC plants discharge DOW water into shallower ocean waters, the transport of large volumes of nutrient-rich DOW to the euphotic zone is inherent. DOW contains many nutrients such as silicon, phosphorus, and nitrogen as well as micronutrients such as nickel and iron that are depleted in the euphotic zone (Pan et al., 2015). When these previously limiting nutrients are introduced into the euphotic zone it stimulates an increase in primary productivity. While this resultant enhanced biological productivity can lead to more natural carbon uptake due

to increased photosynthesis in areas of artificially induced upwelling, it will also result in greater numbers of biota undergoing the previously mentioned processes such as entrainment and impingement.

Chemical

The sea surface pH will increase from the addition of CO_2 to ocean surface waters as CO_2 levels in the atmosphere increase from anthropogenic emissions. As more CO_2 is added to surface waters, the carbonate species equilibrium is shifted. This equilibrium shift results in fewer aqueous bicarbonate ions. Bicarbonate is a weak base and an important constituent of alkalinity. Alkalinity is the capacity of water to resist acidification. When the amount of bicarbonate decreases, there are fewer available ions to resist acidification. This then raises alkalinity and pH, creating a positive feedback loop where ocean acidification increases. The implementation of OTEC results in a slower decrease in surface ocean alkalinity, in part due to the elevated photosynthesis which results from increased primary productivity. The addition of high alkalinity DOW to surface waters by OTEC upwelling also slows the decrease in alkalinity.

As mentioned in the biological section, the artificially induced upwelling from OTEC water discharge will bring many nutrients into the euphotic zone. Due to the resultant increase in biomass and primary productivity, there will be an increase in oxygen production. Sea surface warming however will directly oppose this effect. Since oxygen becomes less soluble as the ocean waters warm, there will be increased oxygen outgassing at the air-sea interface.

3.3.2 The Cost of OTEC

The cost to build OTEC plants varies greatly depending on the location, scale, and technology used to build these plants. At this time there is limited quantitative cost data available for OTEC, with most cost references based on feasibility studies from limited sources including

Lockheed Martin and Vega (Kempener and Neumann, 2014). The capital cost of OTEC is often reported in USD / kW. In 2014 Kempener and Neumann attempted to provide an overview of the available cost projections for a range of OTEC plants, spanning in capacity from 5 to 250 MW (Fig. 8). They found that due to the large overhead cost, small scale (those capable of producing less than 10 MW power) OTEC plants have comparatively higher capital costs / kW than larger (10 to 100 MW) OTEC plants do.

Based on their work, the capital cost of an OTEC plant with 100 MW capacity would range from USD_{2010} 5,000 / kW to 15,000 / kW. Therefore for an OTEC plant with 100 MW capacity, the capital cost per 100 MW OTEC plant would be USD_{2010} 5 million to 15 million. These capital costs include plant components such as vertical pipes, pumps, heat exchangers, and components for thermodynamic cycles, which are considered predictable costs since these components are commercially available for other offshore operations. Other costs, such as labour, were estimated based on USD_{2010} prices (Kempener and Neumann, 2014).

Kempener and Neumann (2014) estimated that CC-OTEC plants are slightly cheaper than open-cycle designs. However, OC-OTEC plants produce fresh water as a by-product and closed-cycle plants do not, so the economic benefits of freshwater production may make OC-OTEC systems more economically viable in the long term, particularly for small island nations. The interest and discount rates, such as government subsidies, have a high impact on cost estimates. Once OTEC is operational, the LCOE in $(USD_{2014} / kWh)^2$ also depends on interest rates and subsidies. As seen in Figure 9 for a 100 MW plant, it is estimated that LCOE could range from 0.07 to 0.19 $(USD_{2014} / kWh)^2$ (Kempener and Neumann, 2014; Vega, 2012; Muralidharan, 2012; Vega, 2007). Additionally, Vega (2012) estimates that using government bonds rather than commercial loans (government loans have a lower interest rate) could reduce

the LCOE of OTEC power generation to around USD_{2014} 0.03 for a 100 MW OTEC plant (Fig. 9).

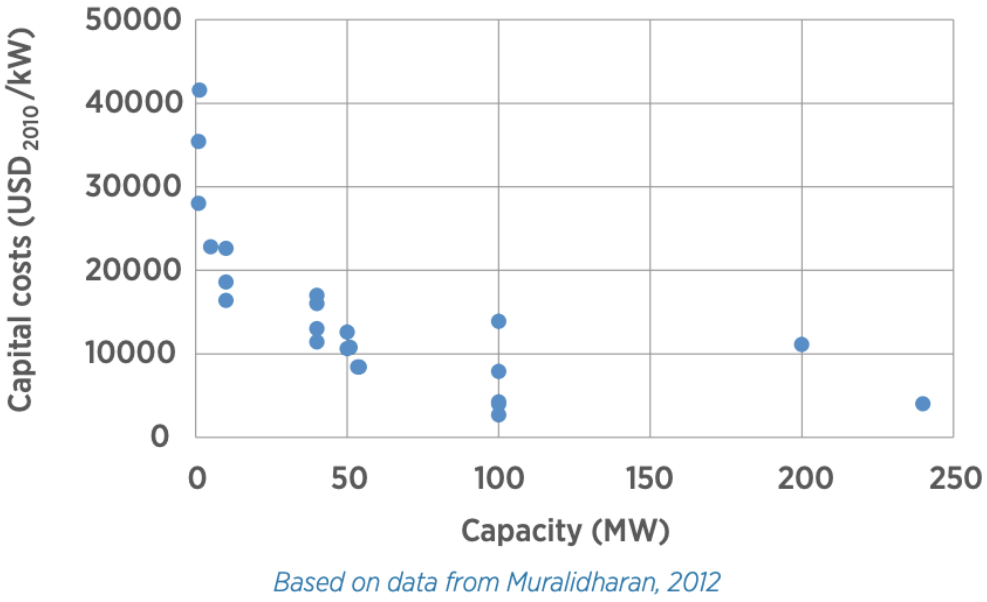

Figure 8: *Graph displaying the capital costs in USD_{2010} / kW for OTEC power plants of varying capacity. Image sourced from Kempener and Neumann (2014).*

	Source of LCOE (USD/kWh)[2]				
Size (MW)	Vega (2007; 2012)[3]	Energy and Environ-ment Council (2011)	Straatman & van Stark (2008)	Upshaw (2012)	Muralidharan (2012)
1-1.35	0.60-0.94	0.51-0.77			
5[4]	0.35-0.65				
10	0.25-0.45	0.19-0.33			
28				0.13-0.65	
50	0.08-0.20	0.10-0.16	0.11-0.32		
50 (combined with offshore solar pond)	0.03-0.05		0.04-0.06		
100	0.07-0.18				0.19
200					0.16
400					0.12

[a] All costs are converted into USD using currency rates at the date of publication.

[b] An 8% interest rate for 15 year loan, annual inflation of 3%, and US labour costs.

[c] Plants smaller than 5 MW of are scheduled to be used in combination with seawater air-conditioning systems, which share in the cost of the infrastructure and provide a significantly lower LCOE from the plant, thus it may not be relevant to show a specific price for this range.

Figure 9: *Image of a table comparing the LCOE cost in* $(USD_{2014} / kWh)^2$ *for OTEC plants of varying capacity from different estimates. Image sourced from Kempener and Neumann (2014).*

4. Methodology

This research was conducted using version 2.9 of the University of Victoria Earth System Climate Model (UVic ESCM). The UVic ESCM is a fully coupled ocean-atmosphere-land surface-sea ice model of intermediate complexity (Weaver et al., 2011). This model is described by Weaver et al. (2001).

4.1 Description of the University of Victoria Earth System Climate Model

The UVic ESCM consists of an energy-moisture balance atmospheric model, a dynamic-thermodynamic sea-ice model (Hibler, 1979; Hunke and Dukowicz, 1997; Bitz et al., 2001) and a primitive equation oceanic general circulation model (Pacanowski, 1995). The UVic ESCM has fully coupled representations of oceanic and terrestrial carbon cycles (Matthews, 2004) and a global coverage with horizontal resolution of 3.6 degrees (zonal) by 1.8 degrees (meridional) (Weaver et al., 2001; Brennan, 2012). The model was spun up for 10,000 years with specified forcing for the year 1850 only varying seasonally. The model was then integrated for another 1250 years with transient-historical forcing (see Eby et al., 2009 for details). Beyond the year 2000, a single run with transient RCP 8.5 forcing (with specified CO_2) was used to diagnose the CO_2 emissions equivalent to those from anthropogenic sources. Beyond the year 2300, year-2300 forcing was specified with only seasonal variation. The diagnosed emissions were then used for all subsequent model simulations. This allowed for the model to react to the sequestration of CO_2 rather than be constrained by specific concentrations.

4.1.1 UVic ESCM Energy-Moisture Balance Atmospheric Model

Atmospheric Model

The UVic ESCM atmospheric model is based on the energy-moisture balance model of Fanning and Weaver (1996) (Weaver et al., 2001). Version 2.9 of the UVic ESCM has a single atmospheric layer that captures the climatic mean state (Matthews, 2004). This atmospheric layer is forced by seasonally varying solar insolation and National Centers for Environmental Prediction (NCEP) reanalysis winds collected daily over 40 years (1958 to 1998) by Kalnay et al. (1996). The thermodynamic energy equations are vertically integrated and assume decreasing specific tracer distributions (heat, moisture, and carbon) with different e-folding scale heights

(Weaver et al., 2001). These e-folding scales are used to decrease the weight of NCEP winds with height for tracer advection. NCEP surface winds are also converted to wind speeds in order to be used in the calculation of sensible or latent heat fluxes between the atmosphere and sea-ice or oceanic general circulation models (Weaver et al., 2001). By including a full annual cycle of solar insolation for past and present orbital configurations, the UVic ESCM can be used for long transient paleoclimate integrations and equilibrium paleo climate applications (Berger, 1978; Weaver et al., 2001).

Vegetation Land Model

The UVic ESCM dynamic vegetation land surface scheme is stimulated by the Top-down Representation of Interactive Foliage and Flora Including Dynamics (TRIFFID) and is a modified variant of the Met Office Surface Exchange Scheme (MOSES) (Breannan, 2012; Essery et al., 2001). This land surface model has a one-layer soil moisture representation which runs off to one of thirty-two rivers (Meissner et al., 2003). Which river is used is based on which river catchment basin the grid cell is located. Snow can build up as a single layer with height variation. The snowmelt can either replenish soil moisture or, once the soil is saturated, contribute to river runoff (Brennan, 2012).

4.1.2 Dynamic-Thermodynamic Sea-Ice Model

The dynamic-thermodynamic sea ice used in the UVic ESCM has two subgrid scale categories: open and ice-covered ocean (Brennan, 2012). The model also employs elastic viscous plastic ice rheology (Hunke and Dukowicz, 1997) and a height-varying sea ice layer. When snow falls on the sea ice it accumulates as a single-height varying snow layer. The sea ice is assumed to have zero heat capacity and therefore is in instantaneous balance with external forcings (MacDougall, 2014). The dynamics of sea ice are simulated using a momentum balance

accounting for the internal deformation of ice as well as ocean and wind stress (MacDougall, 2014). This dynamic-thermodynamic model for sea ice is further described by Bitz et al. (2001).

4.1.3 Oceanic General Circulation Model

The Oceanic General Circulation Model (OGCM) is based on the Geophysical Fluid Dynamics Laboratory Modular Ocean Model 2.2 (Pacanowski, 1995) and the Navier Stokes equations of fluid motion (with Boussinesq and hydrostatic approximations) (MacDougall, 2014). The OGCM has 19 vertical layers with varying thicknesses, ranging from 50 metres at the ocean surface to 518 metres at the bottom ocean layer (Weaver et al., 2001). The ocean is forced by surface buoyancy and surface wind stress fields.

The Ocean Carbon Cycle

The UVic ESCM ocean carbon cycle has modules for ocean biology, inorganic carbon chemistry, and carbonate sediment deposition and dissolution. The atmospheric-ocean flux of CO_2 is driven by the difference in partial pressure of surface ocean CO_2 and atmosphere CO_2 (MacDougall, 2014). Ocean biology is stimulated using a simple marine ecosystem model created by Schmitterner et al. (2008). By including ocean biology, the UVic ESCM can simulate the biological pump, the alkalinity pump, ocean anoxia, and (along with terrestrial biology) global net primary productivity. The marine ecosystem includes: two types of phytoplankton, nitrogen fixing and non-nitrogen fixing, that grow based on temperature, nutrient availability, and light availability; zooplankton, that consume phytoplankton; and detritus from phytoplankton and zooplankton that sinks to the ocean floor. Calcium carbonate ($CaCO_3$) is treated as an ocean tracer and moves through the marine biota, being taken up by phytoplankton, before transforming into a fixed fraction of detritus and transported to the ocean floor.

Upon oceanic dissolution, CO_2 moves to equilibrium with other species of dissolved inorganic carbon. Dissolved inorganic carbon is treated as a passive tracer and moves throughout the ocean following ocean circulation. This results in very little carbon being held as aqueous CO_2. The carbonate sediment deposition and dissolution module takes into consideration the slow feedback between carbonate sediment dissolution and ocean pH. When there is more CO_2 in the atmosphere, the ocean-atmosphere exchange results in increased aqueous CO_2. This lowers oceanic pH, therefore changing the stability of $CaCO_3$ and increasing the rate of dissolution of oceanic calcite sediments. This dissolution in turn releases more carbonate anions into the ocean. In the UVic ESCM, this process is simulated by using an oxygen-only model of sediment respiration based on the work of Archer (1996) (MacDougall, 2014).

4.2 Modelled OTEC Description

To determine useful OTEC plant locations, the UVic ESCM considers the temperature gradient present in each viable ocean grid cell and OTEC plant placement is prioritised in locations where there is the greatest temperature gradient. This is because OTEC is most efficient in the areas with the greatest temperature gradient. OTEC requires a thermal gradient of at least 18ºC between the level where the SOW uptake occurs (at 25-metre depth) and the DOW uptake occurs (at 1,000-metre depth) (Nihous, 2005). If the temperature gradient falls below 18ºC the OTEC plant will be decommissioned and relocated.

In this experiment, water was set to travel through the OTEC pipes with a radius of 10 metres at 1 metre per second. Each OTEC plant had one pipe for SOW uptake, one pipe for DOW uptake, and one pipe for discharge. Water discharge occurs at 25-metre depth and was approximated as a conical plume with a radius of 500 metres. The number of OTEC plants built is a function of the number of plants that can be constructed in a given year, the number of plants

needed to meet the requested power demand, the area remaining in each grid cell, and the temperature gradient in each grid cell. OTEC plants will be built until their construction capacity is exceeded, there are enough plants to meet the specified power demand, the temperature gradient is reduced below 18ºC everywhere, or there is no area left for new OTEC plants. OTEC plants were modelled with a minimum 100 square kilometres around plants in order to avoid overcrowding, which could rapidly deplete the thermal gradient.

The OTEC plant placement is considered unstable when there is more total power requested from the OTEC plants than can be produced. This is because the temperature gradient is depleted faster than it can be replenished by DOW movements. This causes plant placement to become unstable. Therefore OTEC plants cannot remain in the grid cell and are forced to relocate every year. The result of this is a highly fluctuating OTEC plant number which when plotted appears as a sawtooth pattern. Each OTEC plant is modelled to generate 100 MW of electricity. This is the typical power output of a commercial-sized OTEC plant (Adiputra et al., 2019; Rocheleau & Grandelli, 2011).

5. Experiment Design

5.1 OTEC Power Requests

The calculated emission reduction was incorporated by factoring it into transient CO_2 atmospheric forcing where all OTEC-generated electricity was used to power DACCS. This can then be modelled to compare emissions as usual to a “business as normal” scenario. In this experiment, the model began OTEC plant production in 2030 and reached the number of plants needed to meet the requested power demand in 2100. The effects were observed from June 30, 2000, to June 30, 2099. In this experiment, the UVic ESCM first built plants in the area with the

highest temperature gradient in the selected areas until the area was filled. This increment placement scheme allowed for plant production to be reproduced and consistently compared across runs.

In this report, two model integrations are compared. Both use diagnosed emissions from IPCC Representative Concentration Pathway 8.5 (RCP 8.5). The IPCC RCPs were used extensively in models run for in the 2014 IPCC Fifth Assessment Report and include a time series of emissions and GHG concentrations from 2005 to 2100 with extensions to 2300 (IPCC, 2018). RCP 8.5 represents a "business as usual" scenario where there are high emissions without effective climate change mitigation practices (IPCC, 2018). In this scenario, the radiative forcing reaches 8.5 W / m^2 by 2100 (IPCC, 2018). Following diagnosed emissions from RCP 8.5 results in a global temperature increase of around 4.3^{o}C and a total of 1225 ppm atmospheric CO_2 by 2099. This results in an average surface temperature of 17.6^{o}C (Fig. 10).

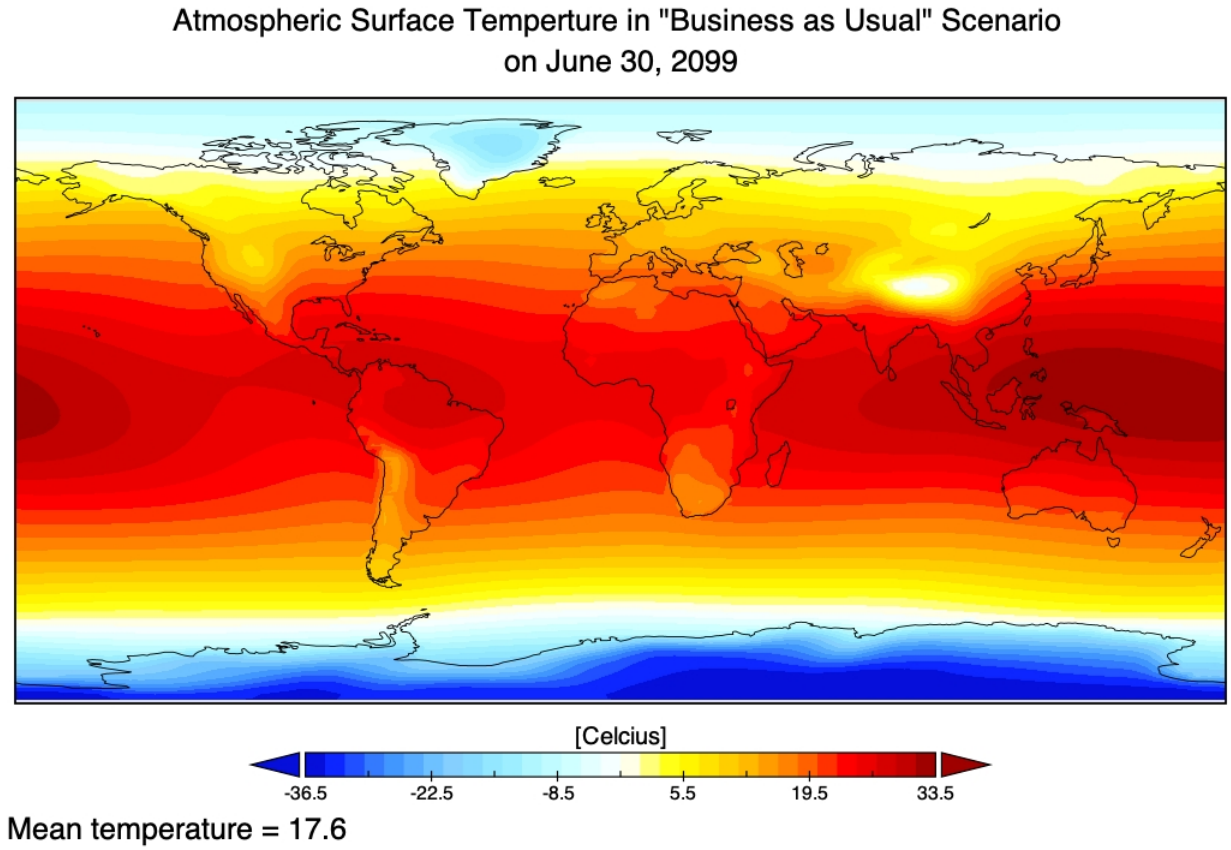

Figure 10: *Atmospheric surface temperature experienced on June 30, 2099 with the "business as usual" scenario based on RCP 8.5 diagnosed emissions with no OTEC or DACCS.*

The first run, Scenario A, is a "business as usual" global warming scenario where there is no OTEC and no DACCS. The second run, Scenario B, uses OTEC to power DACCS. In Scenario B OTEC power plant production begins on July 1, 2030 and increases in a raised negative cosine function to peak at 3 TW energy produced on June 30, 2099. This is a fairly significant amount of electricity, as in 2019 the global consumption of energy was 13.2 TW (International Energy Agency, 2021). When 3 TW of OTEC generated electricity is all directed into DACCS approximately 19.6 Gt CO_2 can be removed from the atmosphere.

A demand of 3 TW of electricity was chosen as the maximum amount of energy OTEC can produce in a year without having widespread negative effects on the ocean. This number is

based on work from Nihous (2006) who recommended 3 TW as the "maximum steady-state OTEC electrical power". While the work of Nihouys (2006) suggests that 5 TW is also sustainable at a steady state, this project considered 3 TW as a safer estimate.

5.2 CO_2 Emissions Reductions

To account for how much DACCS could occur when powered by 3 TW of OTEC, emissions reductions were considered to be a direct factor of OTEC power. This was done using the work of Keith et al. (2018) where 366 kWh is needed to capture and sequester one tonne of CO_2 (Eq. 2).

$$(3 \times 10^{12}\ W)\left(\frac{1\ tonne\ CO_2}{366{,}000\ Whr}\right)\left(\frac{12.011\ g/mol\ C}{44.01\ g/mol\ CO_2}\right)\left(\frac{8760\ hr}{1\ yr}\right)\left(\frac{10^3\ kg}{1\ tonne}\right)\left(\frac{1\ Gt}{10^{12} kg}\right) = 19.596\ Gt\ C\ /\ yr \quad \text{(Eq. 2)}$$

5.3 Selected Geologic Sites

The two sites selected for this project are 1. off the east coast of Oman in the Arabian Ocean and 2. off the Northern coast of Venezuela (Fig. 11). Both sites are excellent target basins for long-term CO_2 storage because of their stability and structural integrity (Benson et al., 2018). This is in large part due to their location on the passive edge of stable continental plates. This and their location close to the equator is why these sites were selected. While there is a large need to obtain more information on the storage capacity of these selected areas, their known large amounts of oil and gas reserves suggest that there would be the capacity to store large amounts of CO_2.

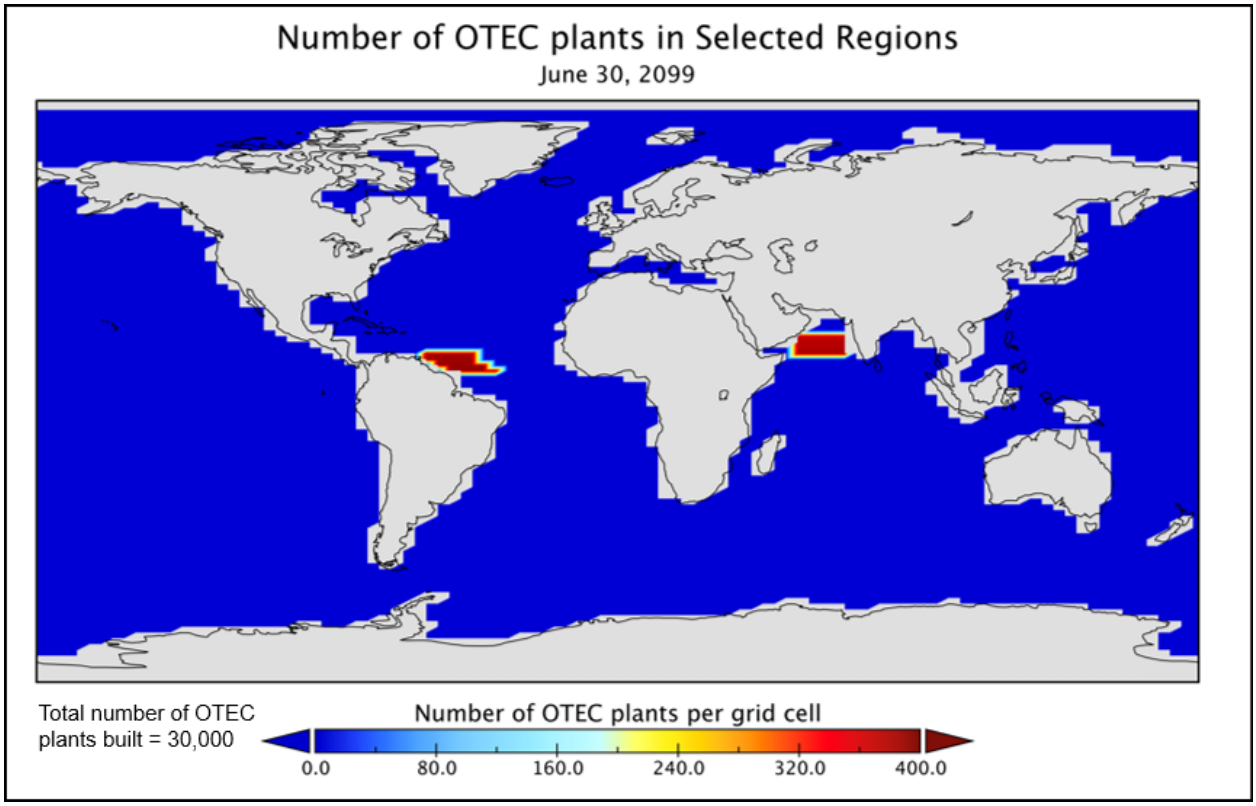

Figure 11: *Map of the selected geologic regions with the number of OTEC plants per grid cell on June 30, 2099.*

6. Results

6.1 Atmospheric CO_2 Reduction

With OTEC power production beginning in 2030 and peaking in 2099 at 3 TW of electricity, approximately 19.6 Gt of CO_2 are sequestered. This is roughly twice the amount of CO_2 emissions calculated for 2030 by using RCP 8.5 diagnosed emissions (11.25 Gt). Using diagnosed emissions from RCP 8.5 global CO_2 emissions reach 24.14 Gt / yr in 2099 in Scenario A (Fig. 12). This correlates to a global atmospheric CO_2 concentration of 922.40 parts per million (ppm) in 2099 (Fig. 13). In Scenario B, global CO_2 emissions continue to increase for about 20 more years, from 2030 to 2050, before beginning to decline. This occurs because OTEC

power production, and therefore the amount of DACCS that can be fueled, increases with time. By 2099 in Scenario B global total CO_2 emissions are 4.56 Gt / yr (Fig. 12). This correlates to a global atmospheric CO_2 concentration of 645.003 ppm in 2099 (Fig. 123.

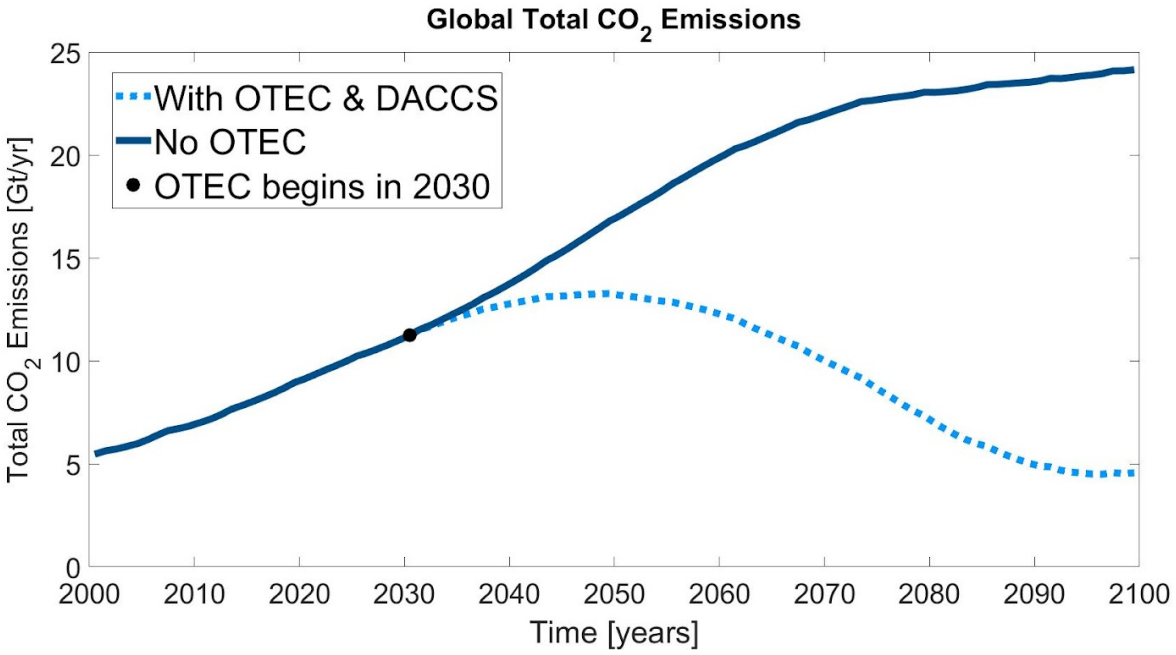

Figure 12: *Global total CO_2 emissions in Gt / yr from June 30, 2000 to June 30, 2099 with two scenarios: one with no OTEC and one with OTEC producing 3 TW of power directed at DACCS. OTEC begins on June 30, 2030.*

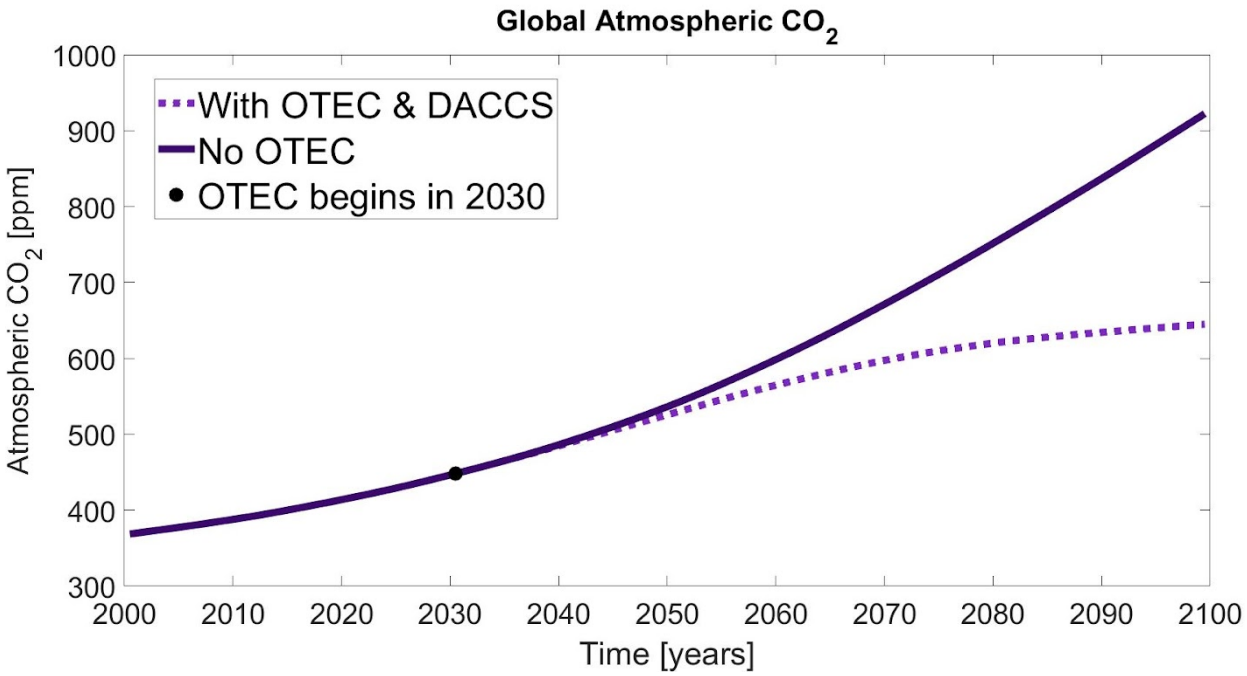

Figure 13: *Global atmospheric CO_2 in ppm from June 30, 2000 to June 30, 2099 with two scenarios: one with no OTEC and one with OTEC producing 3 TW of power directed at DACCS. OTEC begins on June 30, 2030.*

6.2 Surface Temperature Mitigation

Reducing global CO_2 levels will mean that global surface temperatures do not rise as much as they otherwise would have. In Scenario A with diagnosed emissions from RCP 8.5, global temperatures hit an average of 17.6ºC in 2099 (Fig. 10, Fig. 14, Fig. 15). In Scenario B with OTEC and DACCS, global temperatures reach an average of 16.4ºC (Fig. 15). Scenario B is 1.18ºC cooler in 2099 than Scenario A. In these scenarios, global temperatures still rise 2.72ºC and 1.54ºC respectively more than the 2030 average global temperature of 14.85ºC. The relative temperature decrease is felt across the globe but is most strongly seen in the areas where OTEC is operational and over the Arctic (Fig. 16).

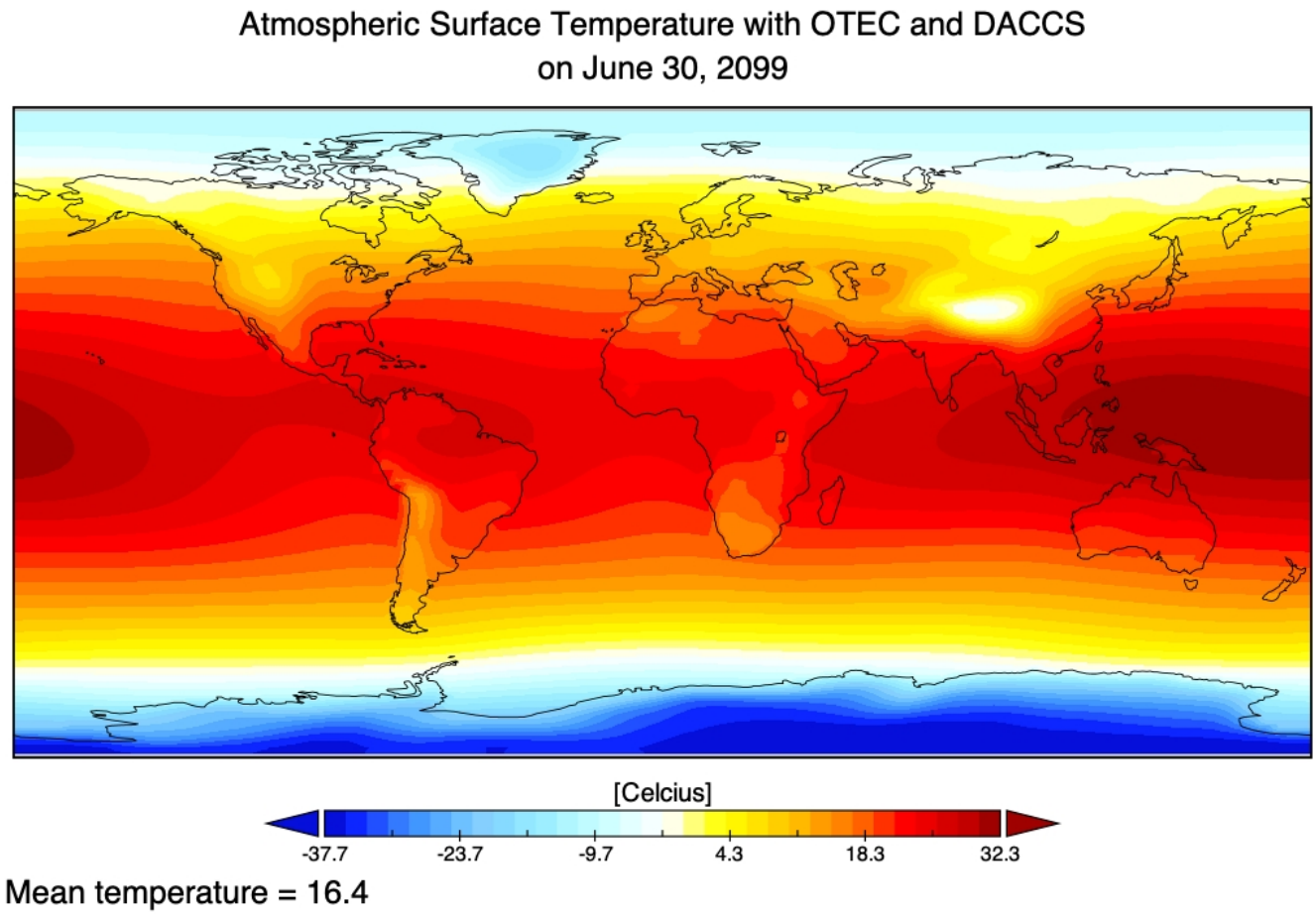

Figure 14: *Atmospheric surface temperature experienced on June 30, 2099 with OTEC producing 3 TW of power directed at DACCS.*

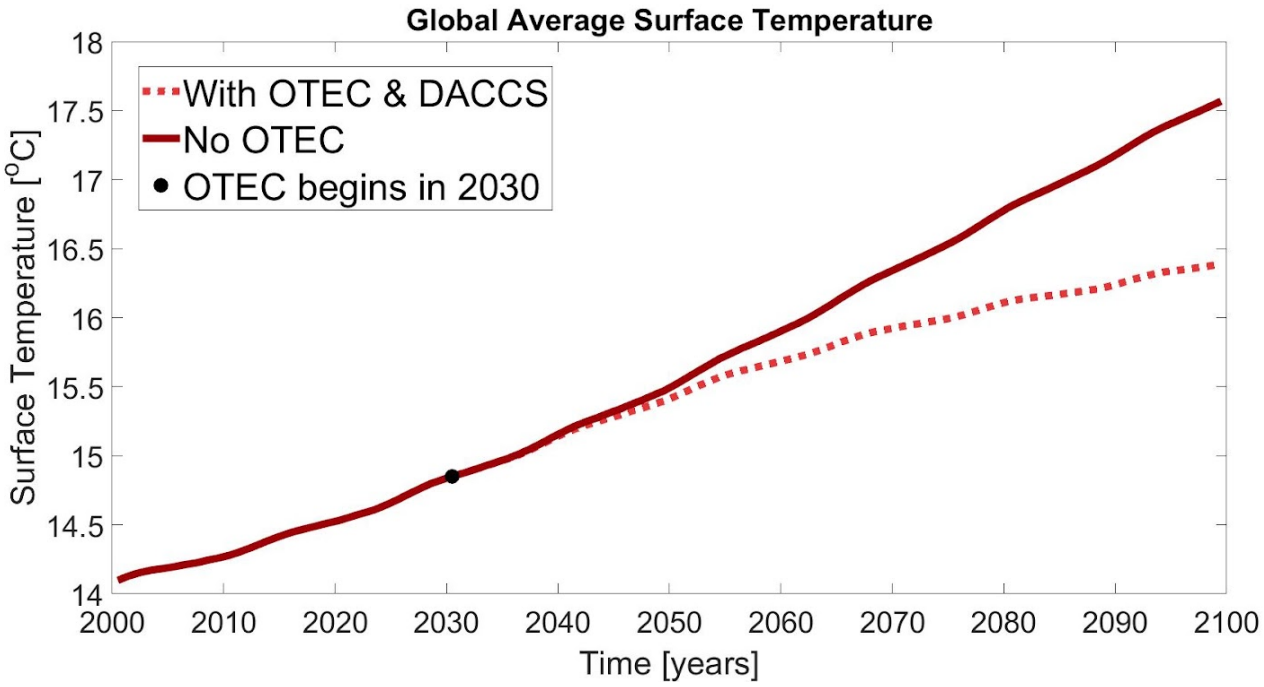

Figure 15: *Global average surface temperature in °C from June 30, 2000 to June 30, 2099 with two scenarios: one with no OTEC and one with OTEC producing 3 TW of power directed at DACCS. OTEC begins on June 30, 2030.*

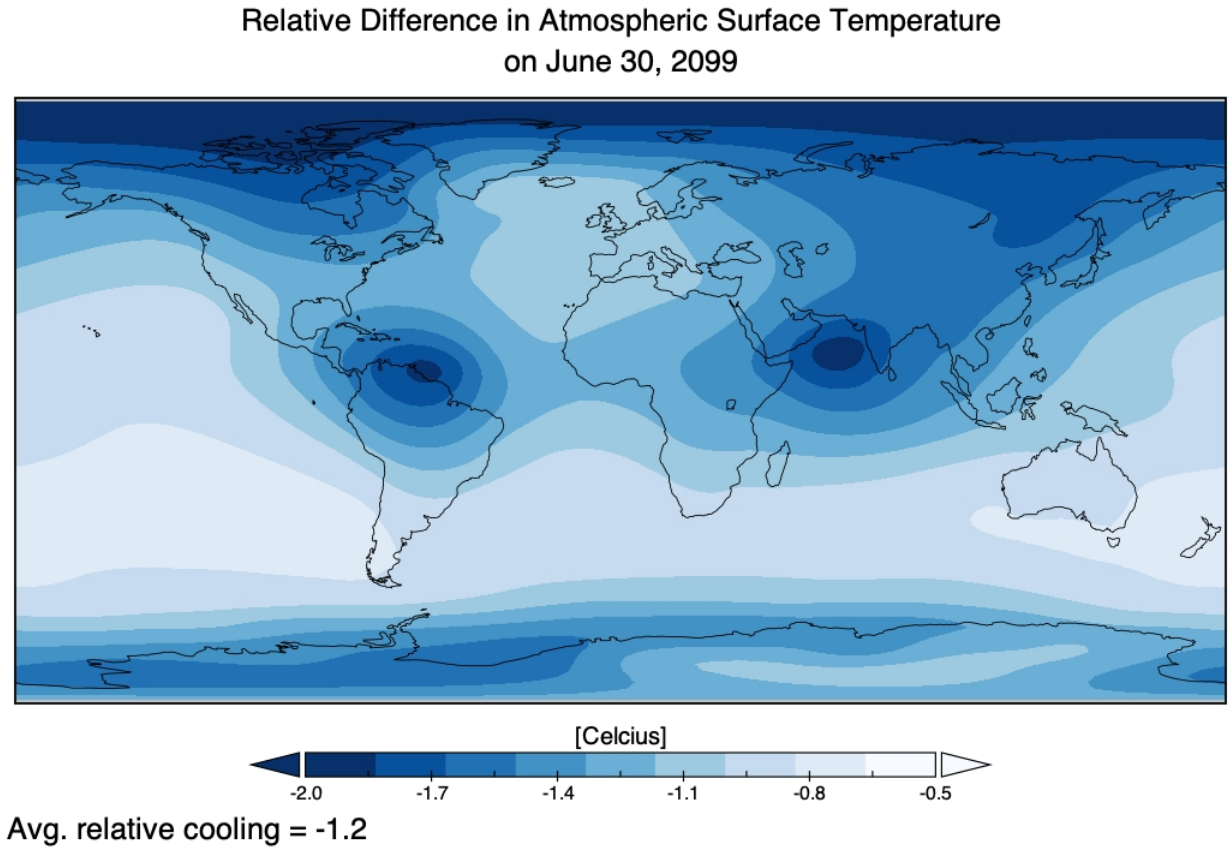

Figure 16: *Global relative surface temperature cooling experienced in ºC on June 30, 2099 through the implementation of OTEC powering DACCS from June 30, 2030 to June 30, 2099. Two scenarios are compared: one with no OTEC and one with OTEC producing 3 TW of power directed at DACCS. OTEC begins on June 30, 2030.*

7. Discussion

7.1 The Use of OTEC to Power DACCS

Most OTEC energy potential is far offshore (Rau and Baird, 2018). Using OTEC as an energy source for in situ negative emissions technology therefore eliminates the energy cost of transporting OTEC produced energy via pipes back to land (Rau and Baird, 2018). OTEC already contributes directly to climate change mitigation as it produces carbon neutral energy while cooling surface water temperatures (Rau and Baird, 2018). While OTEC has not been

deployed to scale, theoretically OTEC could replace most fossil fuel based energy and be deployed continuously on an almost indefinite basis (GESAMP, 2019; Rau and Baird, 2018).

7.2 Comparison of CO_2 Emissions Mitigation

In 2018 the World Energy Outlook predicted that global yearly CO_2 emissions by 2040 will be in the range of 17.6 to 42.5 Gt CO_2 (Cozzi et al., 2018). Both ocean and land CO_2 sinks are struggling to keep up with the rate of anthropogenic CO_2 emissions (Friedlingstein et al., 2022). If global emissions continue at the current rate, NOAA estimates that by 2100 ocean surface water could reach a pH of 7.8. The current average ocean surface pH is around 8.1; the last time ocean surface pH was at 7.8 was during the mid-Miocene 14 to 17 million years ago when the Earth was several degrees warmer and major terrestrial and aquatic extinctions occurred (Raup and Sepkoski, 1984).

7.3 Comparison of Temperature Mitigation

As of 2023, human activities are highly likely to have caused around 1.1ºC of global warming since the pre-industrial period (Masson-Delmotte et al., 2022; Shukla et al., 2022). The observed global mean surface temperature from 2006 to 2015 was approximately 0.87ºC higher than that of 1850 to 1900 (Masson-Delmotte et al., 2022). The present trend of global warming is the average of 30 years, centred on 2017 and assuming the 2018 rate of global warming continues (Masson-Delmotte et al., 2022). If the 2018 global rate of warming of around 0.2ºC per decade continues, global warming is very likely to reach 1.5ºC above pre-industrial levels between 2030 and 2052 (Masson-Delmotte et al., 2022). Even if anthropogenic emissions were halted today, warming from these emissions will cause long term changes to the climate system and likely increase global warming by at least an additional 0.6ºC (Masson-Delmotte et al.,

2022). Given that greenhouse gases will remain in the atmosphere for decades to come, it is unavoidable that climate-related risks for human and natural systems, including sea level rise and extreme weather intensification, will be felt globally Masson-Delmotte et al., 2022).

While some of these impacts, such as the loss of certain ecosystems, are unstoppable and irreversible, if further warming and climate-related risks are to be prevented then both sustained negative emissions technologies and reductions to GHG radiative forcing are required (Masson-Delmotte et al., 2022; Smith et al., 2015; Pielke et al., 2009). While there will still be dramatic environmental changes with a 1.5ºC global temperature increase, this number can be used as the baseline for a realistic limit on global warming (de Coninck et al., 2018). If global warming gradually stabilises at 1.5ºC, the aggregate of climate related risks is less than if global warming exceeds 2ºC and reaches a peak temperature before returning to 1.5ºC. Since these climate related risks will continue to aggregate as warming rises, the level of risk depends on the duration, peak, and rate of warming (Masson-Delmotte et al., 2022).

8. Conclusion

As long as the thermocline is not depleted, OTEC could be deployed on an almost infinite basis (GESAMP, 2019). This would create a substantial source of carbon neutral or carbon negative energy, and theoretically replace most fossil fuel based energy (Muralidharan, 2012). With OTEC implementation is the tropics making the tropical ocean surface temperatures slightly cooler, this may help decrease the strengthening of tropical storms that are seen as a result of anthropogenic climate change (Lau, 2016).

OTEC power production to the low level of 3 TW of electricity a year can result in the long-term removal of significant amounts of atmospheric CO_2 and cooler surface temperatures

than would otherwise occur. A temperature reduction of 1.18ºC caused by 3 TW of OTEC generated electricity powering DACCS is a significant mitigation technique. This temperature mitigation can be compared to the about 1.1ºC temperature increase that has been experienced since the pre-industrial times in the 1850s. This temperature decrease has led to numerous changes that species are struggling to adapt to in a short time, including extreme weather event intensification, habitat loss, sea level rise, ice sheet melt, and rapid alterations to global biogeochemical cycles (Dhakal et al., 2022). There are potential negative impacts to implementing OTEC on a large scale including changes in ocean temperatures, biological productivity, precipitation patterns, and atmosphere-ocean variability. While these must be considered, this combination of green energy and negative emission technology offers an exciting new approach to help mitigate anthropogenic climate change.

9. References

1. Avery, W. H., and Wu, C. (1994). Renewable energy from the ocean: a guide to OTEC. *Ser. Johns Hopkins University Applied Physics Laboratory Series in Science and Engineering. Oxford University Press.*
2. Benson, S., Cook, P., Anderson, J., Bachu, S., Nimir, H. B., Basu, B., et al. (2018). Underground Geological Storage: IPCC Special Report on Carbon Dioxide Capture and Storage. *Working Group III of the Intergovernmental Panel on Climate Change.* https://www.ipcc.ch/site/assets/uploads/2018/03/srccs_chapter5-1.pdf.
3. Berger, Andrél. (Dec. 1978). Long-Term Variations of Daily Insolation and Quaternary Climatic Changes. *J. of the Atmos. Sci.*, **35**(12), 2362-2367. https://doi.org/10.1175/1520-0469(1978)035<2362:LTVODI>2.0.CO;2.
4. Bitz, C. M., and Lipscomb, W.H. (1999). An Energy-Conserving Thermodynamic Model of Sea Ice. *J. Geophys. Res.: Oceans*, **104**(C7). 15669-15677. https://doi.org/10.1029/1999JC900100.
5. Bolles, D. (16 March, 2023). Climate Variability. *National Aeronautics and Space Administration.* https://science.nasa.gov/earth-science/oceanography/ocean-earth-system/climate-variability.
6. Brennan, C. E. (2012). Modelling Oxygen Isotopes in the UVic Earth System Climate Model under Preindustrial and Last Glacial Maximum Conditions: Impact of Glacial-Interglacial Sea Ice Variability on Seawater D18O. *University of Victoria.* https://dspace.library.uvic.ca/handle/1828/4261.

7. Carbon Engineering Ltd. (2023). Direct Air Capture and Storage of CO2. *Carbon Engineering*. https://carbonengineering.com/direct-air-capture-and-storage/.
8. Celia, M. A., Bachu, S., Nordbotten, J. M., Bandilla, K. W. (30 July 2015). Status of CO2 Storage in Deep Saline Aquifers with Emphasis on Modelling Approaches and Practical Simulations. *Water Resources Research*, **51**(9). 6846-6892. https://doi.org/10.1002/2015WR017609.
9. Chadwick, R.A., Arts, R., Eiken, O. (2005). 4D seismic quantification of a growing CO2 plume at Sleipner, North Sea. In: A.G. Dore and B. Vining (eds.), Petroleum Geology: North West Europe and Global Perspectives - Proceedings of the 6th Petroleum Geology Conference. *Petroleum Geology Conferences Ltd.*
10. Cozzi, L., Gould, T., Gul, T., Wanner, B., Bouckaert, S., McGlade, C., et al. (2018). World Energy Outlook 2018. *International Energy Agency*. https://iea.blob.core.windows.net/assets/77ecf96c-5f4b-4d0d-9d93-d81b938217cb/World_Energy_Outlook_2018.pdf.
11. d'Arsonval, J. (1881). Utilisation des forces naturelles, avenir de l'électricité. *Le Revenue Scientifique*, **17**, 370-372.
12. de Coninck. H., Revi., A., Babiker, M., Bertoldi, P., Buckeridge, M., Cartwright, A., et al. (2018). Strengthening and Implementing the Global Response. In: Global Warming of 1.5°C. An IPCC Special Report on the impacts of global warming of 1.5°C above pre-industrial levels and related global greenhouse gas emission pathways, in the context of strengthening the global response to the threat of climate change, sustainable development, and efforts to eradicate poverty [Masson-Delmotte, et al.]. *Cambridge University Press,* 313-444. doi:10.1017/9781009157940.006.

13. Devault, D. A. and Péné-Annette, A. (Nov. 2017). Analysis of the Environmental Issues Concerning the Deployment of an OTEC Power Plant in Martinique." *Environ. Sci. Pollut. Res.*, **24**(33), 25582–601. https://doi.org/10.1007/s11356-017-8749-3.

14. Dhakal, S., Minx, J. C., Toth, F. L., Abdel-Aziz, A., Figueroa Meza, M. J., Hubacek, K., et al. (2022) Emissions Trends and Drivers. In IPCC, 2022: Climate Change 2022: Mitigation of Climate Change. Contribution of Working Group III to the Sixth Assessment Report of the Intergovernmental Panel on Climate Change [P.R. Shukla, J. Skea, R. Slade, A. Al Khourdajie, R. van Diemen, D. McCollum, M. Pathak, S. Some, P. Vyas, R. Fradera, M. Belkacemi, A. Hasija, G. Lisboa, S. Luz, J. Malley, (eds.)]. *Cambridge University Press*. doi: 10.1017/9781009157926.004.

15. Eskander, S. M. S. U. and Fankhauser, S. (Aug. 2020). Reduction in Greenhouse Gas Emissions from National Climate Legislation. *Nat. Clim. Change,* **10**(8), 750-756. https://doi.org/10.1038/s41558-020-0831-z.

16. Eby M., Zickfeld K., Montenegro A., Archer D., Meissner K. J., Weaver A. J. (2009). Lifetime of Anthropogenic Climate Change: Millennial Time Scales of Potential CO2 and Surface Temperature Perturbations. *J. Climate*, **22**, 2501–2511. https://doi.org/10.1175/2008JCLI2554.1.

17. Essery, R., Best, M., Cox, P. (14 Aug. 2021). *MOSES 2.2 Technical Documentation. Hadley Centre technical note 30.* https://jules.jchmr.org/sites/default/files/HCTN_30.pdf.

18. Faizal, M. and Ahmed, M. R. (March 2013). Experimental Studies on a Closed Cycle Demonstration OTEC Plant Working on Small Temperature Difference. *Renew. Energ.*, **51**, 234–40. https://doi.org/10.1016/j.renene.2012.09.041.

19. Friedlingstein, P., O'Sullivan, M., Jones, M. W., Andrew, R. M., Gregor, L., Hauck, J., et al. (11 Nov. 2022). Global Carbon Budget 2022. *Earth Syst. Sci. Data*, **14**(11), 4811–900. https://doi.org/10.5194/essd-14-4811-2022.

20. Gasda, S. E., Bachu, S., Celia, M. A. (2004), Spatial characterization of the location of potentially leaky wells penetrating a deep saline aquifer in a mature sedimentary basin, *Environ. Geol.*, **46**(6–7), 707–720.

21. GESAMP. (2019). High level review of a wide range of proposed marine geoengineering techniques. *IMO/FAO/UNESCO-IOC/UNIDO/WMO/IAEA/UN/UN Environment/ UNDP/ISA Joint Group of Experts on the Scientific Aspects of Marine Environmental Protection.* (98), 144. http://www.gesamp.org/publications/high-level-review-of-a-wide-range-of-proposed-marine-geoengineering-techniques.

22. Gingerich, P. D. (30 Jan. 2019). Temporal Scaling of Carbon Emission and Accumulation Rates: Modern Anthropogenic Emissions Compared to Estimates of PETM Onset Accumulation. *Paleoceanography and Paleoclimatology*, (34). 329-335. https://doi.org/10.1029/2018PA003379.

23. Hibler, W. D. (July 1979). A Dynamic Thermodynamic Sea Ice Model. *Journal of Physical Oceanography*, **9**(4), 815-846. https://doi.org/10.1175/1520-0485(1979)009<0815:ADTSIM>2.0.CO;2.

24. Horn, F. L. and Steinberg, M. (May 1982). Control of Carbon Dioxide Emissions from a Power Plant (and Use in Enhanced Oil Recovery). *Fuel*, **61**(5), 415-422. https://doi.org/10.1016/0016-2361(82)90064-3.

25. House, K. Z., Baclig, A. C., Ranjan, M., Herzog, H. J. (5 Dec. 2011). Economic and Energetic Analysis of Capturing CO2 from Ambient Air. *Env. Sci.*, **108**(51), 20428–33. https://doi.org/10.1073/pnas.1012253108.

26. Hunke, E. C. and Dukowicz, J. K. (1 Sep. 1997). An Elastic–Viscous–Plastic Model for Sea Ice Dynamics. *J. Phys. Oceanogr.* **27**(9), 1849-1867. https://journals.ametsoc.org/view/journals/phoc/27/9/1520-0485_1997_027_1849_aevpmf_2.0.co_2.xml.

27. International Energy Agency. (15 Oct. 2021). Key World Energy Statistics 2021. *Organisation for Economic Co-operation and Development.* https://www.oecd-ilibrary.org/energy/key-world-energy-statistics-2021_2ef8cebc-en.

28. IPCC. (2018). IPCC DDC Glossary. *IPCC.* https://www.ipcc-data.org/guidelines/pages/glossary/glossary_r.html.

29. Johnson, F. A. (1992). Closed-Cycle Ocean Thermal Energy Conversion. *American Society of Civil Engineers,* (5), 70–96.

30. Johnson, K., Martin, D., Zhang, X., DeYoung, C., Stolberg, A. (2017). Carbon Dioxide Removal Options: A Literature Review Identifying Carbon Removal Potentials and Costs. *University of Michigan*. http://deepblue.lib.umich.edu/handle/2027.42/136610.

31. Kalnay, E., Kanamitsu, M., Kistler, R., Collins, W., Deaven, D., Gandin, L., et al. (1 March 1996). The NCEP/NCAR 40-Year Reanalysis Project. *Bulletin of the American Meteorological Society*, **77**(3), 437–72. https://doi.org/10.1175/1520-0477(1996)077<0437:TNYRP>2.0.CO;2.

32. Keith, D. W., Holmes, G., St. Angelo, D., Heidel, K. (15 Aug. 2018). A Process for Capturing CO2 from the Atmosphere. *Joule*, **2**(8), 1573–94. https://doi.org/10.1016/j.joule.2018.05.006.

33. Kempener, R. and Neumann, F. (June 2014). Ocean Thermal Energy Conversion Technology Brief. *International Renewable Energy Agency*. https://www.irena.org/-/media/Files/IRENA/Agency/Publication/2014/Ocean_Thermal_Energy_V4_web.pdf.

34. Klusman, R.W. (2003). A geochemical perspective and assessment of leakage potential for a mature carbon dioxide-enhanced oil recovery project and as a prototype for carbon dioxide sequestration; Rangely field, Colorado. *American Association of Petroleum Geologists Bulletin*, **87**(9), 1485–1507.

35. Lackner, K. S. (11 Nov. 2016). The Promise of Negative Emissions. *Science*, **354**(6313), 714–714. https://doi.org/10.1126/science.aal2432.

36. Lackner, K. S., Brennan, S., Matter, J. M., van der Zwaan, B. (27 July 2012). The Urgency of the Development of CO2 Capture from Ambient Air. *Proceedings of the National Academy of Sciences*, **109**(33), 13156-13162. https://doi.org/10.1073/pnas.1108765109.

37. Laul, J. (2016). Cost effective OTEC (ocean thermal energy conversion) electrical power plant. *MIT Center for Collective Intelligence.* https://www.climatecolab.org/contests/2015/harnessing-the-power-of-mit-alumni/c/proposal/1325332.

38. Le Quéré, C., Korsbakken, J. I., Wilson, C., Tosun, Andrew, R., Andres, R. J., et al. (25 Feb. 2019). Drivers of Declining CO2 Emissions in 18 Developed Economies. *Nature Climate Change*, **9**(3), 213-217. https://doi.org/10.1038/s41558-019-0419-7.

39. MacDougall, A. H. (2014). A Modelling Study of the Permafrost Carbon Feedback to Climate Change: Feedback Strength, Timing, and Carbon Cycle Consequences. *University of Victoria.* https://dspace.library.uvic.ca/bitstream/handle/1828/5422/MacDougall_Andrew_PhD_2014.pdf?sequence=4&isAllowed=y.

40. Masson-Delmotte, V., Zhai, P., Portner, H., Roberts, D., Skea, J., Shukla, P. R., et al. (2022). Global Warming of 1.5°C: IPCC Special Report on Impacts of Global Warming of 1.5°C above Pre-Industrial Levels in Context of Strengthening Response to Climate Change, Sustainable Development, and Efforts to Eradicate Poverty. *Cambridge University.* https://doi.org/10.1017/9781009157940.

41. Masutani, S. and Takahashi, P. (2000). Ocean Thermal Energy Conversion. In Encyclopedia of Electrical and Electronics Engineering. *Wiley,* 93-103.

42. Matthews, H. D. (2004). Land Cover Change, Vegetation Dynamics and the Global Carbon Cycle : Experiments with the UVic Earth System Climate Model. *University of Victoria.* https://dspace.library.uvic.ca/handle/1828/484.

43. Metz, B. O., Davidson, O., de Coninck, H. C., Loos, M., Meyer, L. A., et al. (2005). IPCC Special Report on Carbon Dioxide Capture and Storage. *Working Group III of the Intergovernmental Panel on Climate Change.* https://www.ipcc.ch/site/assets/uploads/2018/03/srccs_wholereport-1.pdf.

44. Moritis, G. (2002). Enhanced Oil Recovery. *Oil and Gas Journal*, **100**(15), 43–47.

45. Muralidharan, S. (2012). Assessment of Ocean Thermal Energy Conversion. *Massachusetts Institute of Technology*. https://dspace.mit.edu/handle/1721.1/76927.

46. Nihous, G. C. (March 2018). A Preliminary Investigation of the Effect of Ocean Thermal Energy Conversion (OTEC) Effluent Discharge Options on Global OTEC Resources. *J. Mar. Sci. Eng.* **6**(1), 25. https://doi.org/10.3390/jmse6010025.

47. Nihous, G. C. (July 2006). A Preliminary Assessment of Ocean Thermal Energy Conversion Resources. *J. Energy Resour. Technol.,* **129**(1), 10–17. https://doi.org/10.1115/1.2424965.

48. Nihous, G. C. (April 2005). An Order-of-Magnitude Estimate of Ocean Thermal Energy Conversion Resources. *J. Energy Resour. Technol.,* **127**(4), 328-333. https://doi.org/10.1115/1.1949624.

49. NOAA. (1 April 2020). Ocean Acidification. *National Oceanic and Atmospheric Administration.* https://www.noaa.gov/education/resource-collections/ocean-coasts/ocean-acidification.

50. Nordbotten, J. M. and Celia, M. A. (2012) Geological Storage of CO2: Modeling Approaches for Large-Scale Simulation. *Wiley.*

51. Pacanowski, R. C. (7 Nov. 1996). MOM 2 Version 2.0 Beta Documentation User's Guide and Reference Manual. *GFDL Ocean Technical Report 3.2.* https://www.gfdl.noaa.gov/wp-content/uploads/2016/10/manual2.2.pdf.

52. Pan, Y., Fan, W., Zhang, D., Chen, J., Huang, H., & Liu, S. et al. (10 Dec. 2015). Research progress in artificial upwelling and its potential environmental effects. *Sci. China Earth Sci.,* **59**(2), 236-248. https://doi.org/10.1007/s11430-015-5195-2.

53. Paynter, D. and Ramaswamy, V. (n.d.) Aerosols and Climate. *Geophysical Fluid Dynamics Laboratory.* https://www.gfdl.noaa.gov/aerosols-and-climate/.

54. Rajagopalan, K. and Nihous, G.C. (Feb. 2013). Estimates of Global Ocean Thermal Energy Conversion (OTEC) Resources Using an Ocean General Circulation Model. *Renewable Energy*, **50**, 532-540. https://doi.org/10.1016/j.renene.2012.07.014.

55. Rau, G.H. and Baird, J. R. (Nov. 2018). Negative-CO2-Emissions Ocean Thermal Energy Conversion. *Renewable and Sustainable Energy Rev.,* **95**, 265-272. https://doi.org/10.1016/j.rser.2018.07.027.

56. Raup, D. M. and Sepkoski, J. J. (Feb. 1984). Periodicity of Extinctions in the Geologic Past. *Proceedings of the National Academy of Sciences of the United States of America*, **81**(3), 801-805.

57. Rumjaun, A. B., Borde, B., Guilyardi, E., Lescarmontier, L., Matthews, R., Niewohner, C., et al. (2018). IPCC Special Report “Global Warming of 1.5°C” Summary for Teachers. *IPCC.* https://www.ipcc.ch/site/assets/uploads/sites/2/2018/12/ST1.5_OCE_LR.pdf.

58. Shukla, P. R., Skea, J., Slade, R., Al Khourdajie, A., van Diemen, R., McCollum, D., et al. (2022). Mitigation of Climate Change. Contribution of Working Group III to the Sixth Assessment Report of the Intergovernmental Panel on Climate Change. *Cambridge University Press*. doi: 10.1017/9781009157926.

59. Skovholt, O. (1993). CO2 Transportation System | PDF | Pipeline Transport | Carbon Dioxide. *Energy Convers. Mgmt.* **34**(9-11), 1095-1103. https://www.scribd.com/document/179066592/Skovholt-1993-CO2-Transportation-System.

60. Socolow, R., Desmond, M., Aines, R., Blackstock, J., Bolland, O., Kaarsberg, T., et al. (1 June, 2011). Direct Air Capture of CO2 with Chemicals A Technology Assessment for the APS Panel on Public Affairs. *APS.* https://www.aps.org/policy/reports/assessments/upload/dac2011.pdf.

61. Stein, T. (3 June, 2022). Carbon Dioxide Now More than 50% Higher than Pre-Industrial Levels. *National Oceanic and Atmospheric Administration.* https://www.noaa.gov/news-release/carbon-dioxide-now-more-than-50-higher-than-pre-industrial-levels.

62. Stevens, S.H., Kuuskra, V. A., Gale, J., Beecy, D. (2001). CO2 injection and sequestration in depleted oil and gas fields and deep coal seams: worldwide potential and costs. *Environ. Geosci.*, **8**(3), 200–209. https://www.usgs.gov/faqs/what-carbon-sequestration.

63. UNFCCC. (2022). *The Paris Agreement*. https://unfccc.int/process-and-meetings/the-paris-agreement/the-paris-agreement.

64. U.S. Department of Energy. (2023). Closed Cycle. *Tethys Engineering*. https://tethys-engineering.pnnl.gov/technology/closed-cycle.

65. US Energy Information Administration. (9 Aug. 2022). Hydropower explained Ocean thermal energy conversion. *US Energy Information Administration.* https://www.eia.gov/energyexplained/hydropower/ocean-thermal-energy-conversion.php.

66. Vega, L. A. (1 Jan. 2016). Ocean Thermal Energy Conversion. *Renew. Energ.* https://doi.org/10.1007/978-1-4614-5820-3_695.

67. Vega, L. A. (2012). Ocean Thermal Energy Conversion. *Encyclopedia of Sustainability Science and Technology*, 7296-7328. https://link.springer.com/referenceworkentry/10.1007/978-1-4419-0851-3_695#citeas.

68. Vega, L.A. (22 Aug. 2007). OTEC Economics, *Offshore Infrastructure Associations*.

69. Vega, L. A. (1999). Ocean Thermal Energy Conversion (OTEC).

70. Vega, L. A. (1995). Ocean Thermal Energy Conversion. *Energy Technology and the Environment*, 2104–2119.

71. Weaver, A. J., Eby, M., Wiebe, E. C., Bitz, C. M., Duffy, P. B., Ewen, T. L., et al. (12 April 2001). The UVic Earth System Climate Model: Model Description, Climatology, and Applications to Past, Present and Future Climates. *Atmosphere-Ocean*. https://www.academia.edu/17004739/The_UVic_earth_system_climate_model_Model_description_climatology_and_applications_to_past_present_and_future_climates.

72. Weaver, A. J., Bitz, C. M., Fanning, A. F., Holland, M. M. (May 1999). Thermohaline Circulation: High-Latitude Phenomena and the Difference between the Pacific and Atlantic. *Annu. Rev. Earth and Planetary Sci.,* **27**, 231-285. https://doi.org/10.1146/annurev.earth.27.1.231.

73. Wei, N., Li, X., Jiao, Z., Stauffer, P. J., Liu, S., Ellett., K., et al. (18 Jan. 2022). A Hierarchical Framework for CO2 Storage Capacity in Deep Saline Aquifer Formations. *Front. Earth Sci.,* **9**. https://www.frontiersin.org/articles/10.3389/feart.2021.777323.

74. Whittaker, S.G. (2005): Geological characterization of the Weyburn Field for geological storage of CO2: Summary of Phase I results of the IEA GHG Weyburn CO2 Monitoring and Storage Project; in Summary of Investigations 2005, Volume 1. *Saskatchewan Geological Survey*.

https://pubsaskdev.blob.core.windows.net/pubsask-prod/88854/88854-Whittaker_2005vol1.pdf.

75. Wood, D. A. and Hazra, B. (13 Oct. 2017). Characterization of Organic-Rich Shales for Petroleum Exploration & Exploitation: A Review-Part 1: Bulk Properties, Multi-Scale Geometry and Gas Adsorption. *J. Earth Sci.*, **28**(5), 739-757. https://doi.org/10.1007/s12583-017-0732-x.
76. World Ocean Review. (2010). Fossil Fuels « World Ocean Review. *World Ocean Review*. https://worldoceanreview.com/en/wor-1/energy/fossil-fuels/. Accessed 6 Jan. 2023.
77. Xue, L., Ma, J., Hu, Q., Cheng, M., Wen, X., Wu, N., et al. (Dec. 2021). Identification of CO2 Leakage from Geological Storage Based on Maize Spectral Characteristic Indexes. *Int. J. Greenh. Gas Control*, **112**, 103342. https://doi.org/10.1016/j.ijggc.2021.103342.
78. Yool, A., Shepard, J. G., Bryden, H. L., Oschlies, A. (21 Aug. 2009). Low efficiency of nutrient translocation for enhancing oceanic uptake of carbon dioxide. *J. Geophys. Res.* vol. 114. https://doi.org/10.1029/2008JC004792.
79. Zhao, W., Chen, Y., Wu, J., Zhu, Z., Wang, J. (Dec. 2021). Study on CO2 Capture Upgrading of Existing Coal Fired Power Plants with Gas Steam Mixture Cycle and Supercritical Water Coal Gasification. *Int. J. Greenh. Gas Control*, **112**, 103482. https://doi.org/10.1016/j.ijggc.2021.103482.
80. Zhou, S., Liu, X., Bian, Y., Shen, S. (15 Aug. 2020). Energy, Exergy and Exergoeconomic Analysis of a Combined Cooling, Desalination and Power System. *Energy Convers. Manag.* **218**, 113006. https://doi.org/10.1016/j.enconman.2020.113006.